SRC 2025

University of Houston

Earth and Atmospheric Sciences

38th Annual Student Research Conference

Thursday, May 8th, 2025

Table of Contents

Schedule..... 5
Oral Presentations..... 6
Poster Presentations..... 10
Keynote Speaker..... 13
Abstracts..... 14
Student Committee..... 46
Judges..... 47
Volunteers..... 48
Acknowledgments..... 49

American Association of Petroleum Geologists (AAPG)
aapg.wildcatters@gmail.com

American Meteorological Society (AMS)
uhstudentams@gmail.com

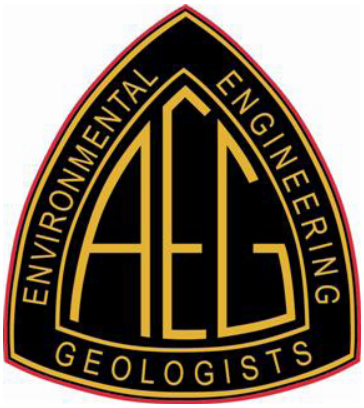

Association of Environmental and Engineering Geologists (AEG) and American Institute of Professional Geologists (AIPG)
AEGatUH2@gmail.com

Geological Society (GeoSociety)
geosocietyatuh@gmail.com

Society of Exploration Geophysicists (SEG) Wavelets
segwavelets@gmail.com

Schedule & Logistics

Check-In & Breakfast	8:30 - 9:30 a.m.
Oral Presentations	9:30 - 10:45 a.m.
Coffee Break	10:45 - 11:00 a.m.
Oral Presentations	11:00 - 12:00 p.m.
Lunch Break	12:00 - 1:00 p.m.
Poster Presentations	1:00 - 3:00 p.m.
Headshots	2:00 - 3:00 p.m.
Keynote Lecture	3:00 - 3:25 p.m.
Awards Ceremony	3:25 - 4:45 p.m.
Group Photo	4:45 p.m.
Happy Hour	5:00 - 7:30 p.m.

Oral Presentations
SR1 Room 223/634
Poster Presentations
All Students:
SR1 2nd, 3rd, and 4th Floors
Headshots
SR1 Room 204D
Keynote Lecture | Awards Ceremony
SR1 Room 117

Oral Presentations

SR1 223

9:30 a.m.

Karissa Vermillion (PhD)

Cenozoic Thermal Evolution of the Western San Gabriel Mountains, southern CA: Insights from Apatite Fission Track Thermal Modeling

9:45 a.m.

Makenna Harris (MS)

How Charcoals Record Grassland Fires in the Stratigraphic Record: A Case Study from the 2024 Windy Deuce Fire in the Texas Panhandle

10:00 a.m.

Isabela Garcia (Undergrad)

Unraveling the seismic history of SW Montana: Implications for hazard along Red Rock fault

10:15 a.m.

Asmara A. Lehrmann (PhD)

Tidally influenced interactions between the glacial grounding zone, substrate, and ocean recorded in channels and small moraines on the seafloor offshore of the Dotson Ice Shelf, Antarctica

10:30 a.m.

Jamie Jetton (Undergrad)

Turbidite Signals in Nearshore Sediments of the Larsen-A Ice Shelf

Oral Presentations

SR1 223

11:00 a.m.

Poorna Srinivasan (PhD)

Compositional and isotopic evaluation of gases generated from hydrous pyrolysis of coal

11:15 a.m.

Nina Zamani (PhD)

Faulty Assumptions: Decoding Seismic Deformation in Carbonates through Mineral Reactions

11:30 a.m.

Sarah Garcia (MS)

Effects of Water Level Fluctuations and Floodplain Inundation on Sediment Deposition and Organic Carbon Burial in the Delta of Elephant Butte Reservoir, New Mexico

11:45 a.m.

Kennedy Potter (Undergrad)

Subaqueous Carbon Sequestration in Elephant Butte Reservoir, New Mexico

Oral Presentations

SR1 634

9:30 a.m.

Andres Galindo (MS)

Thermal Evolution and Source Rock Maturity Assessment of the Mahanadi Basin, India Using 1D Basin Modeling

9:45 a.m.

Shawn Fields (MS)

Provenance and Paleogeography of the Vantage Sandstone, Central Washington, USA

10:00 a.m.

Fnu Anshika (PhD)

Method development for analysis of Phthalate emissions (plastic additives) in air using comprehensive two-dimensional gas chromatography

10:15 a.m.

Nabeel Muhammedy (MS)

Investigating the Mechanical Properties of Aletai Meteorite

10:30 a.m.

Hadi Zanganeh Kia (PhD)

High-Resolution CFD Framework for Urban Air Pollution Modeling

Oral Presentations

SR1 634

11:00 a.m.

Semko Momeni (PhD)

Unlocking Uncharted Territory: The First Satellite-Based Assessment of Ammonia Emissions Over Open Water

11:15 a.m.

Oussama Romdhani (PhD)

The Role of Turbulence Parametrization in Convective Self-Aggregation over the Greater Houston Area

11:30 a.m.

Breno Goldenberg Araujo (MS)

Differentiating turbidites and contourites in a Miocene-Pleistocene deep-water drift deposit, offshore West Antarctica

11:45 a.m.

Alexei Ignatiev (MS)

Cretaceous opening of the Canada Basin (High Arctic): New Constraints from regional gravity and magnetic data

Poster Presentations
2nd Floor

1 Nirvan Abhilash (PhD) | *Physics-Informed Neural Networks for Rainfall Nowcasting : A Hybrid Data-Physics Approach*

2 Amna Afzal (PhD) | *Microplastic Detection in Complex Environmental Matrices: Comparative Study of Thermal Degradation Methods*

3 Jumoke Akinpelu (PhD) | *Crustal structure characterization offshore Niger Delta, Nigeria: impact on hydrocarbon exploration in ultra-deepwater*

4 Claudia Aramburu Tinoco (Undergrad) | *Monitoring Spatiotemporal Variability of Suspended Sediment in Texas Coastal Systems Using In-Situ Measurements and Hyperspectral Imaging*

5 Muhammad Asif (PhD) | *Constraining Orogen-Parallel Extension in the Central Himalayas: Insights from InSAR Time-Series on the Dangardzong Fault*

6 Tarryn Aucamp (PhD) | *Unraveling Olympus Mons: Lava Flows, Surface Evolution and Geologic Mapping*

7 Ruth Beltran (PhD) | *Crustal structure and structural evolution of the Brazilian rifted passive margin in the Campos basin, Brazil*

8 Kyra Bennett (MS) | *A chemometric machine learning framework for oil classification: A California case study*

9 Ashish Bhattarai (PhD) | *Evaluating WRF-CAMx Model Performance in Simulating Surface Ozone During Different Sky Conditions in Houston, Texas*

10 Nathaniel Brunello (Undergrad) | *Investigations into the deformation history of the Cutoff Formation, SE New Mexico.*

11 Abigail Cantoni (PhD) | *Detrital zircon from Mars: trapped sediment components in the highly shocked shergottite northwest Africa 11509*

13 Patrick Casbeer (MS) | *Manganese phase identification and oxidation state assessment in analog sample analysis at Mars-evolved gas analyzer measurements*

14 Juan Cruz (Undergrad) | *Investigating SWS Parameters Preceding the 2009 Mw 6.1 L'Aquila Earthquake*

15 Rijul Dimri (PhD) | *Graph Neural Network-based PM2.5 concentration estimation and forecasting*

16 Amberlee Enger (MS) | *Using Isotope Forensics to Solve the Case of Carbonation and Serpentinization of Modern Oceanic Peridotites from the Vavilov Basin, Mediterranean Sea*

17 Morgann Farley (Undergrad) | *Sediment Budget Investigation of Longyearelva in Longyearbyen, Svalbard*

18 Zachary Guess (MS) | *A Critical Evaluation of the Young Moon Hypothesis: Radiogenic Ca and Sr isotope constrains on the contentious relationship between anorthosite and pyroxenite lithologies in 60025*

Poster Presentations 3rd Floor

19 Nilay Gungor (PhD) | *Seismic Insights into Deep-Water Stratigraphy and Reservoir Potential in the Mahanadi Basin, India*

20 Rashik Islam (PhD) | *Deep Learning-Based PM Forecasting and Post-Infant Mortality Assessment in Urban Areas: A Case Study in Bangladesh*

21 Sui Jia (PhD) | *Metamorphic history and detrital provenance of the Torbashi thrust sheet, Eastern Pamir, and their tectonic significance*

22 Sagun Gopal Kayastha (PhD) | *A Deep Learning Framework for Satellite-Derived Surface PM 2.5 Estimation: Enhancing Spatial Analysis in the United States*

23 Nima Khorshidian (PhD) | *Investigating Aerosol–Cloud Interactions over Houston Using Advanced WRF-Chem Schemes*

24 Emily Klang, Avery Narhi (Undergrad) | *An Investigation of the Aeolian Transport Mechanisms That Form Lomas in the Rio Grande Delta*

25 Raymond Kwaku Twumasi Oware (PhD) | *Evaluating E3SM Global Storm-Resolving Model Simulations of Deep Convection: Insights from DP-SCREAM during TRACER*

26 Syd Lineberry (Undergrad) | *Using Thermochronology to understand fault movement, with special consideration of the Granite Pass fault, Little Hatchet Mountains, NM*

27 Melania D. Maqway (PhD) | *The Isola Dike, Northwest Italy: Evidence for Carbonatite Metasomatism in the Lower Continental Crust of the Ivrea-Verbano Zone (IVZ), Southern Alps*

28 Daniel Maya (PhD) | *Crustal structure and basin modeling of Cretaceous source rocks in deepwater settings*

29 Jack McLaughlin (MS) | *Evaluating the Use of Clay and Groundwater Chemistry to Differentiate Fluvial Versus Marine Sediments in an Oil Field Setting, Focused on the Frio Formation of the Texas Gulf Coast*

Poster Presentations
4th Floor

30 Joshua Miller (MS) | *3D seismic stratigraphy and tectonic controls on contourite and turbidite sedimentation along the deepwater Atlantic margin of Uruguay*

31 Pauline Nguyen (Undergrad) | *Assessing Organic Carbon Pools in Coastal Prairie Soils*

32 Oriyomi Ojelabi (MS) | *Shallow subsurface mapping of Evergreen Cemetery using non-invasive geophysical methods*

33 Abe Okayli Masaryk (PhD) | *Deep earthquakes and association with carbonate equilibrium melting conditions*

34 Jake Parsons (PhD) | *Seismic monitoring of underground hydrogen storage*

35 Anuska Pudasaini (PhD) | *Fingerprinting Meltwater Facies in Pleistocene to Recent Sediments in the Amundsen Sea, West Antarctica*

36 Ali Raza (PhD) | *Decoding stalagmites composition — a non destructive approach*

37 Robby Reyna (MS) | *Applying machine learning techniques to the classification of groundwater contamination within a natural carbon dioxide reservoir*

38 Estefani Ruiz Toro (MS) | *Tectonic origin of the Bering Sea from geophysical and geological constraints*

39 Bilge Sasmaz (MS) | *Development of Mechanical Earth Model and Stress Analysis at the HFTS-1 Site, Midland Basin*

40 Margaret Sauer (Undergrad) | *U-Pb Calcite Geochronology and Fluid Inclusion Analysis of the Earp Formation: Insights into Laramide Deformation in the Little Hatchet Mountains, SW New Mexico*

41 Peter Savrides (MS) | *Crustal structure, tectonostratigraphy, and hydrocarbon potential of the deepwater, rifted-passive margin of Nova Scotia*

42 Kenneth Shipper (PhD) | *Regional maturation model for hydrocarbons along the Guyana-Suriname margin based on improved estimates of the thickness and thermal structure of the rifted lithosphere*

43 Kaylin Tunnell (PhD) | *Mineral chemistry of olivine from chondritic meteorite compared to Martian and 4-Vesta meteorites – implications for the evolution of extra-terrestrial rocky bodies*

44 Md Upal Shahriar (PhD) | *Geophysical insights into tectonostratigraphic framework and hydrocarbon prospectivity in the Andaman Basin*

45 Eugenia Velasco (MS) | *Comparing two data filtering methods to differentiate between on-road vehicle plumes and background measurements*

46 Haini Wang (PhD) | *Re-estimating Moisture Source Contribution Anomalies in the 2011 Texas Extreme Drought Event Using the Two-Layer Dynamic Recycling Model (2L-DRM)*

47 Zhixiang Zhang (PhD) | *A Real-Time Instrument for Monitoring Strain Variations*

Dr. Will Struble
Keynote Speaker

Dr. Will Struble is a hillslope geomorphologist who studies the evolution of steep, tectonically active landscapes where landslides and debris flows are common. His research focuses on quantifying how surface processes record signals of tectonics and climate in the landscape. He also investigates the mechanisms that trigger bedrock landslides – particularly during earthquakes and major storms – and explores the role of forests in mitigating slope failures.

"Landslides and Landscapes: Decoding surface processes to reveal tectonics, climate, and hazards"

3:00 - 3:25

Oral Presentations - SR1 223

Karissa Vermillion (PhD)

Cenozoic Thermal Evolution of the Western San Gabriel Mountains, southern CA: Insights from Apatite Fission Track Thermal Modeling

Here, we present apatite fission track (AFT data from five clasts of the early Miocene Vasquez Formation and analyze these data alongside previously published AFT data from correlative source basement in the western San Gabriel Mountains (Blythe et al., 2000. The western San Gabriel Mountains in southern California preserves the transition from Late Cretaceous-Paleogene shallow subduction to development of the SAFS. The clasts have two populations: three samples were cooler than 150 C since the Late Cretaceous and the other two were hotter than 150 C until ~70 Ma. The older population have over dispersed ages and were likely derived from a slow cooling, upper crustal cap that was exhumed first before the younger population. This upper crustal cap is likely not preserved in the basement, given how thermal modeling of all western San Gabriel basement samples show rapid cooling between 80-40Ma. The younger clast population also shows rapid cooling between 50-30 Ma. Discrepancies between the older clast population and the basement/young clast population can be attributed to structural discontinuities. Comparison between clasts and correlative basement show at least one kilometer of missing removement during rapid exhumation, and another two removed during burial post deposition of the Vasquez Formation. Both basement and clast samples show reheating to temperatures of 60-80 C post Vasquez Formation deposition, correlating with a burial depth of at least 3 kilometers. A second episode of rapid cooling at ~6 Ma brought these samples from 60-80 C to the surface and is likely related to the establishment of the modern SAFS and ongoing restraining bend in the San Gabriel Mountains. This shows the entire San Gabriel Mountains was uplifted ca. 6 Ma, although basement thermochronology only records this event in the eastern San Gabriel Mountains.

Makenna Harris (MS)

How Charcoals Record Grassland Fires in the Stratigraphic Record: A Case Study from the 2024 Windy Deuce Fire in the Texas Panhandle

Wildfires play a crucial role in shaping landscapes by influencing sediment transport and deposition. Understanding post-fire sediment dynamics is essential for reconstructing past fire events and predicting future landscape responses. However, the processes governing sediment and charcoal transport in low-slope (<11o) environments remain poorly understood, particularly in large, post-fire depositional systems. This study will show how post-fire sediment and charcoal transport following the 2024 Windy Deuce Fire in the Texas Panhandle varies across depositional environments within a source-to-sink system, reflecting multiple transport mechanisms. The fire burned in the Lake Meredith National Recreation Area including the hilllopes of McBride Canyon (source) and along the Canadian River and Lake Meredith (sink). Finer silts and clays dominate low-energy lacustrine settings, while coarser sands prevail in high-energy river deltas. Higher %OM in distal lake sediments suggests more stable organic accumulation in deeper waters. Charcoal particle size and morphology distributions confirm the presence of fire-derived material throughout the stratigraphic record, with larger, elongated fragments likely representing high-energy transport and smaller, irregular pieces reflecting deposition under calmer conditions. The range in charcoal sizes and morphologies suggests multiple transport processes, including both fluvial and eolian transport. These findings improve our understanding of post-fire sediment dynamics in low-slope environments, providing insight into how fire signals are recorded in sedimentary archives. This research contributes to paleofire reconstructions by identifying factors that influence the preservation, reworking, and transport of fire-derived materials.

Oral Presentations - SR1 223

Isabela Garcia (Undergrad)

Unraveling the seismic history of SW Montana: Implications for hazard along Red Rock fault

The Intermountain Seismic Belt (ISB) is an area of high seismic risk located in the Rocky Mountains. Its northern section extends through Yellowstone National Park (YNP) into southwestern Montana and southern Idaho where two notable large earthquakes struck: the 1983 magnitude 6.9 Borah Peak earthquake and 1959 magnitude 7.3 Hebgen Lake earthquake. In 2023, YNP was the 4th most visited national park in the United States, exposing large populations to earthquake-related hazards. Seismic risk maps show this entire region to be at high risk; however, the risk remains under-constrained along the seismically active Red Rock fault (RRF). To evaluate potential size of a future earthquake, geologic mapping and field surveys using a real-time kinematic (RTK) GNSS system to obtain high resolution topographic profiles were conducted to estimate age of last rupture for different areas along the RRF. Fault scarp profiling results give rupture ages ranging from 30 to 3 ka, suggesting there has been multiple slip events. Topographic swath profile analysis over a 1m digital elevation model was used to estimate length-displacement along strike, with the goal of determining if accommodation zones inhibited rupture. Rupture scenario calculations indicate there is risk of a 6.5 magnitude earthquake, which would produce widespread ground shaking and soil liquefaction in areas with unconsolidated sediments. Moreover, a large earthquake event on the RRF could trigger another earthquake on an adjacent fault by transferring stress. Infrastructure like dams, hospitals, and highways such as I-15, which facilitates tourism and commerce, are vulnerable to intense shaking; damage could negatively impact local economies. This study concludes the RRF to be a young, active normal fault with high seismic risk, highlighting the need for geologically informed planning.

Asmara A. Lehrmann (PhD)

Tidally influenced interactions between the glacial grounding zone, substrate, and ocean recorded in channels and small moraines on the seafloor offshore of the Dotson Ice Shelf, Antarctica

Glaciers flowing into the Amundsen Sea, Antarctica, are thinning and retreating at an accelerating rate, contributing to global sea-level rise. The retreat of the Amundsen Sea glaciers, including the Dotson Ice Shelf, largely stems from the advection of relatively warm Circumpolar Deep Water (CDW) contacting the grounding zone. Daily tidal pumping of the ice shelves can trap CDW within the grounding zone, leading to accelerating retreat.

By including geologic archives, the short observational record of glacial behavior, such as tidal modulation of the grounding zone, can be extended into longer timescales. For instance, the daily retreat from tidal modulation can be recorded in retreat moraines. However, we have a very limited understanding of the grounding zone as it is nearly impossible to reach.

Here, we present high-resolution data collected during an ITGC cruise, NBP2202, using the Hugin AUV, Ran. Evidence of such retreat ribs offshore Dotson Ice Shelf is overlain by previously unobserved features, which we interpret as small grounding zone channels. The channels crosscut the ribbed retreat ridges and are crosscut by them, indicating contemporaneous formation and, thus, association of the channels with the grounding zone.

We hypothesize that the distinct pattern of channels, parallel to the grounding zone and perpendicular to the glacial flow, has a formation mechanism related to the ribbed features. In this interpretation, excess water is forced out parallel to the ridges as part of the daily tidal cycle that controls the formation of the ribbed retreat ridges. The channelized water flows perpendicular to ice into large glacially carved bathymetric troughs, where the channels terminate in deeper water.

Oral Presentations - SR1 223

Jamie Jetton (Undergrad)

Turbidite Signals in Nearshore Sediments of the Larsen-A Ice Shelf

The 1995 and 2002 CE collapses of the Larsen-A and Larsen-B Ice Shelves on the northeastern Antarctic Peninsula have been linked to accelerated glacial flow and increased sediment discharge into adjacent embayments. Following ice shelf disintegration, the tributary glaciers accelerate in the absence of buttressing and are recorded as turbidites. Such deposits reflect sediment pulses triggered by glacial destabilization or mass transport associated with grounding line retreat. Because of difficulty of access, the stratigraphic record of these events near former grounding lines remains underexplored.

Here, we investigate a marine sediment core, NBP1203_JC21, collected 8 km from the present-day Larsen-A shoreline to evaluate the sedimentary record of the Larsen-A and Larsen-B collapses, and whether similar events occurred in the past. We hypothesize that turbidites are preserved and can be linked to high-energy depositional events from past episodes of grounding line retreat and ice-shelf collapse. Preliminary analyses of magnetic susceptibility, bulk density, core photographs, and X-radiographs indicate the presence of turbidite deposits.

Turbidite sequences produced by such events would provide stratigraphic markers of ice shelf collapse and glacier response, standing out from the more continuous sandy and stratified silty background deposits typical of ice-proximal Larsen-A cores. We will use radioisotope dating and laser particle size analysis to confirm the origin and timing of these deposits. Identifying turbidites in this core will help constrain the timing and magnitude of sediment remobilization tied to ice shelf collapse and grounding line retreat in the Larsen-A sector and can provide context for understanding other glaciers in danger of rapid collapse.

Poorna Srinivasan (PhD)

Compositional and isotopic evaluation of gases generated from hydrous pyrolysis of coal

Monitoring gas emissions from coal formations provides vital information for exploration of hydrocarbon gases and is also important for determining CO2 sequestration sites and evaluating the potential for alternative energy sources like hydrogen. Laboratory experimental techniques, like hydrous pyrolysis (HyPy), can help predict the type and volume of gases generated naturally in the subsurface, but at much shorter timescales.

This current study investigates the change in gas composition and carbon isotopes from an orthohydrous lignite to assess the influence of time and temperature on natural gas generation. HyPy experiments were conducted in a 250 mL pressure vessel using a lignite sample from the Fort Union Formation in Montana. Twenty-four experiments were conducted between 260 °C and 365 ° C and held isothermally for 24-, 72-, and 144-hours. The collected gases were analyzed using gas chromatography (GC) and isotope ratio mass spectrometry (IRMS) techniques.

The experimental run time had a notable effect on both the concentration and carbon isotopes of generated gases. The resultant hydrocarbon gas yields generally increased with increasing thermal maturity, and exponentially increased ~340 °C, likely due to secondary cracking. The 144-hr experiments generated the highest concentration of gases. The experimental run times produced different isotopic trendlines for all the gases, indicating that gas generation is influenced by time. For CO2, increasing the run time resulted in a positive shift of the isotopic trendlines, but the opposite was observed for CH4.

Gas generation is highly dependent on the original organic content, accessory minerals, and simultaneous reactions occurring during thermochemical maturation. Experiments will next be conducted on shales to evaluate the gas yield, composition, and isotopic variability. The results will be compared with the current coal experiments to assess the influence of time and temperature on generation and kinetics.

Oral Presentations - SR1 223

Nina Zamani (PhD)

Faulty Assumptions: Decoding Seismic Deformation in Carbonates through Mineral Reactions

Frictional heating induces critical thermal transformations in carbonate rocks during seismic slip events and hence are fundamental to earthquake mechanics and fault dynamics. >95% of the energy released during seismic is dissipated by frictional heat concentrated at the fault planes which substantially modifies earthquake mechanics. Under rapid heating conditions (<10 seconds carbonate rocks are more susceptible to thermal decomposition (decarbonation resulting in massive production of carbon dioxide (CO_2 a pressurized gas works as lubricant This decline in friction can thus allow for very high rupture velocities, producing supershear ruptures, and strongly determines the earthquake's magnitude and structural damage.

By integrating field data (in situ measurements, thermal models experimental and numerical modelling with multi-dimensional geochemical characterization and Rock-Eval pyrolysis to estimate heat dissipated, quantity and intensity of frictional heating in carbonate fault zones can be quantified. Mineralogical studies of natural faults record a spectrum of friction-generated transformations ranging from thermally destabilized pyrite to dehydrated goethite and transformed hematite to the ultimate decarbonation of calcite, dolomite and siderite. These processes also generate diagnostic secondary minerals, e.g portlandite and nanocalcite that in turn become thermal markers of historic and prehistoric seismic events.

Improved insight into frictional heating processes, mechanisms, and mineralogical changes in carbonate rocks under seismic conditions will help enhance theoretical models of earthquake rupture and mechanics. Moreover, these findings are of great importance for the development of better methodologies for seismic hazard assessment as well as earthquake risk mitigation, thus having meaningful implications for both scientific studies and practical implementations in the fields of geosciences and earthquake engineering.

Sarah Garcia (MS)

Effects of Water Level Fluctuations and Floodplain Inundation on Sediment Deposition and Organic Carbon Burial in the Delta of Elephant Butte Reservoir, New Mexico

In response to severe droughts in the Western U.S., reservoirs provide irrigation and municipal water but lose up to 2% capacity annually due to sedimentation from sparse vegetation and erodible soils. These reservoirs also sequester organic matter (OM), burying ~0.15 PgC/year, nearing oceanic carbon burial rates. This study examines sediment and carbon sequestration in the Elephant Butte Reservoir (EBR) delta on the Rio Grande, New Mexico. The EBR delta accumulates sediment rapidly due to monsoon flooding and snowmelt, functioning as an organic carbon (OC) sink. Lake levels influence OC dynamics: high water submerges the delta, promoting sediment and OM deposition, while low levels expose sediments, potentially releasing OC as CO_2. We assess OC storage and release using remote sensing and field data. Inundation frequency was mapped using the Normalized Difference Water Index on Landsat images. Sediment samples (up to 60 cm deep) were collected across inundation gradients. Loss on ignition estimated OM content, and a laser particle size analyzer assessed grain size. We hypothesize that carbon content correlates with inundation frequency; areas with less flooding likely contain lower OC due to reduced deposition and increased remobilization. Understanding inland reservoirs' role in OC sequestration is crucial for assessing their impact on the global carbon cycle.

Oral Presentations - SR1 223

Kennedy Potter (Undergrad)

Subaqueous Carbon Sequestration in Elephant Butte Reservoir, New Mexico

The American West is a semi-arid region that relies on inland reservoirs for water management. Despite covering less than 2% of the Earth's surface, inland waters bury ~0.15 Pg C/year of terrestrially-derived organic carbon (OC), compared to oceans which bury ~0.20 Pg C/year. In southern New Mexico, the Rio Grande flows into Elephant Butte Reservoir (EBR) delivering sediment-laden, organic-rich water. These sediments build a delta and generate hyperpycnal plumes that drive sediment and OC deep into the reservoir. This research aims to quantify subaqueous carbon storage at EBR, providing insight into the importance of semi-arid inland reservoirs as carbon sinks. In March 2024, we conducted a boat-based campaign to collect conductivity, temperature, and depth data (CTD), water samples, and sediment samples. CTD data were used to determine the presence of hyperpycnal plumes, while water samples were filtered to determine suspended sediment concentration (SSC). Sediment samples were analyzed for grain size distribution and organic matter content (OM%). Although no hyperpycnal plumes were detected, we observed a decline in SSC with increasing distance from the delta and found a mean OM% of 7.5%. Using this OM% in combination with known storage capacity loss, we estimated a carbon burial rate (CBR) of 2029 gC/m^2yr, which exceeds previous estimates based on incoming sediment flux. This indicates that primary production (PP) is likely a significant contributor to OM% within the reservoir, estimated to be ~1242 gC/m^2yr. Our estimated CBR exceeds those reported for similarly-sized global reservoirs, most of which do not account for arid and semi-arid reservoirs systems. These findings highlight the need for further research into carbon sequestration in inland reservoirs of arid regions and the important role of primary production in these environments.

Oral Presentations - SR1 634

Andres Galindo (MS)

Thermal Evolution and Source Rock Maturity Assessment of the Mahanadi Basin, India Using 1D Basin Modeling

The Mahanadi Basin, located offshore eastern India, is a promising basin with significant hydrocarbon potential. This study integrates well log data, source rock evaluation, and seismic interpretation to assess the thermal maturity and transformation ratio (TR%) of key stratigraphic intervals using 1D basin modeling in PetroMod. The analysis focuses on the MND5 and MND6 wells, combining burial history, temperature modeling, and vitrinite reflectance (%Ro) calibration to reconstruct the basin's thermal evolution. Geochemical data, including Total Organic Carbon (TOC), Hydrogen Index (HI), and Tmax, were compiled from ten wells to classify kerogen types and maturity stages. Passey's ΔLogR method was used for TOC estimation, and results were validated against available lab measurements. MND5 reached peak oil window maturity with Ro values of 0.6–1.3% and TR values between 20–60%, while MND6 remained within early maturation stages, with lower temperatures and transformation ratios. Seismic interpretation of 2D lines enabled the mapping of key reflectors and the correlation of picked horizons with stratigraphic boundaries. The image below illustrates a 3D seismic section with interpreted horizons and well paths, including MND-5 highlighting structural features that may influence source rock burial and preservation. These integrated results demonstrate that the lower Cretaceous and Paleocene source rocks reached the oil window due to sufficient burial and thermal conditions, particularly in the deeper parts of the basin. This study supports ongoing exploration efforts by refining understanding of source rock maturity distribution.

Shawn Fields (MS)

Provenance and Paleogeography of the Vantage Sandstone, Central Washington, USA

The Columbia River Basalt Group (CRBG) eruptions spanned ~11 Ma and covered ~210,000 km2 of the Pacific Northwest (PNW) in flood basalts. Of these eruptions, the Grande Ronde Basalt (GRB) eruptions spanned ~ 458 kyr and were the most voluminous, comprising ~72 % of the total CRBG basalt volume. The GRB flows altered the course of the ancestral Columbia River and pushed it westward, towards the Cascades. A ~80-120 kyr period of volcanic quiescence followed the emplacement of the GRB. The Vantage Member of the Ellensburg Formation includes sedimentary interbeds deposited during this period on the largely sediment-free Columbia Plateau. The impact of the voluminous and extensive GRB flows on the ancient drainage systems is not well understood in terms of sediment contributions from arc volcanism to the west and continental margin materials from north of the plateau. This study aims to better understand these relative contributions as represented in fluvial sediments of the Vantage Member which can discriminate main-channel from tributary channel deposits and aid in refining paleo-drainage network maps. We will analyze Vantage Member samples exhibiting fluvial facies characteristics for their framework grain components and their detrital zircon ages. Initial results show clear detrital zircon age differences between arc-derived lahars and paleo-Columbia River deposits. Vantage-aged arc-derived lahars show a relatively unimodal concentration of zircon ages at ~16 Ma whereas paleo-Columbia River deposits contain zircons with ages from ~50 Ma to 2.6 Ga. We believe the Miocene Columbia River zircon signature reflects a combination of material sourced from older continental material such as the Belt Supergroup and younger, metamorphosed material of northern Washington.

Oral Presentations - SR1 634

Fnu Anshika (PhD)

Method development for analysis of Phthalate emissions (plastic additives) in air using comprehensive two-dimensional gas chromatography

Phthalates are semi-volatile organic compounds that are used as plastic additives which get released from plastics throughout their lifecycle. They are known as endocrine disruptors and have adverse impact on neural and reproductive system. This research focuses on developing a method for analysis of phthalates using comprehensive two-dimensional gas chromatography with mass spectrometer (GCxGC/MS) and its distribution in Houston. Multiple combinations of detectors have been tested to develop a method which performs best across all the detectors. The combinations that have been tested are GC-MS, GCxGC/MS, GC-MSMS, gas chromatography with flame ionization detector (GC-FID), GCxGC/FID. The samples will be collected in dust phase, gas-phase and particulate phase. The sampling is currently being conducted across various location in Houston such as traffic signals and highways. This study will be able to provide a comprehensive view over phthalates and improve the understanding of distribution of traditional phthalates and their replacements.

Nabeel Muhammedy (MS)

Investigating the Mechanical Properties of Aletai Meteorite

Meteorites provide a window into the composition and history of our solar system. This study investigates the mechanical properties of the Aletai Iron Meteorite, a rare IIIE-an (anomalous) group meteorite first discovered in 1898 in Xinjiang, China. The research aims to characterize its mechanical properties to evaluate its structural integrity and anisotropic behavior. Using an oscilloscope-based experimental setup, P and S wave arrival times were analyzed to determine elastic wave velocities. MATLAB was utilized for signal visualization and analysis, ensuring precise interpretation of the meteorite's response under stress. The results indicate weak anisotropy in the sample and reveal high bulk modulus values, suggesting it would make for a suitable landing site for future extraterrestrial sample collection missions.

The mechanical behaviour of materials can be characterized through their elastic moduli, which quantify how a material deforms elastically under applied forces. Elastic moduli are calculated by analyzing stress and strain along three axes. In this study, elastic wave velocity and bulk density measurements are used to determine elastic moduli through non-destructive methods.
The results indicated high bulk and shear modulus values, suggesting that the Aletai meteorite has a structurally robust composition. Weak anisotropy was observed, implying minimal directional dependency in its elastic properties. Future work will include analyzing the sample under varying temperature and pressure conditions to determine the behaviour of the meteorite in spatial environment where temperatures tend to be at extremes (lows and highs). and determining other physical properties e.g., porosity, thermal conductivity etc. Obtaining measurements of additional samples will help to see consistency and accuracy of the method.

Oral Presentations - SR1 634

Hadi Zanganeh Kia (PhD)

High-Resolution CFD Framework for Urban Air Pollution Modeling

This study presents a novel Computational Fluid Dynamics (CFD) framework for simulating air pollution dispersion at ultra-fine spatial resolutions—up to 1 meter—within complex urban environments. The model is specifically designed to capture pollutant transport and accumulation near buildings, roadways, and freeways, incorporating the dynamic influence of vegetated areas such as green walls, trees, and roadside greenery. By integrating realistic urban geometries and high-resolution meteorological inputs, the framework bridges the gap between mesoscale air quality models and localized exposure assessments. The simulation captures micro-scale turbulence, building wake effects, and vegetation-induced deposition and flow alterations, offering new insights into pollutant hotspots and mitigation strategies. This framework has significant applications in urban planning, health risk assessment, and environmental policy, enabling stakeholders to evaluate intervention scenarios with unprecedented spatial detail.

Semko Momeni (PhD)

Unlocking Uncharted Territory: The First Satellite-Based Assessment of Ammonia Emissions Over Open Water

Reducing uncertainty in ammonia (NH_3) emissions, particularly those over open water, which have largely been unexplored, remains a key challenge. This study refines 2019 NH_3 emissions over the south-central United States (SCUS) using inverse modeling technique with Cross-track Infrared Sounder (CrIS) data and assesses its impact on inorganic PM_2.5. For the first time, we demonstrate the potential of refining NH_3 emissions over open water using satellite data, specifically over the northwestern Gulf of Mexico (NWGOM). Over NWGOM, average NH_3 concentrations increased significantly by 1.4 ppb, predominantly driven by biological nitrogen fixation. This study highlights the potential of satellite data to refine NH_3 emissions over open water and emphasizes the role high-resolution regional inverse modeling in improving air quality forecasts and global emission estimates.

Oussama Romdhani (PhD)

The Role of Turbulence Parametrization in Convective Self-Aggregation over the Greater Houston Area

Deep convection plays a crucial role in the Earth's climate system by driving large-scale weather patterns and influencing energy and moisture redistribution in the atmosphere. Convective self-aggregation (CSA) refers to the spontaneous organization of convective clouds into large-scale, coherent structures, a phenomenon critical to understanding tropical and subtropical rainfall patterns. However, accurately modeling CSA remains a challenge in part, due to the complexities of sub-grid turbulent processes, which are not fully resolved in many cloud resolving models (CRM). To improve turbulence parametrization, a comprehensive understanding of convective boundary layer dynamics — including small-scale eddies, mixing processes and feedback mechanisms — and their role in the development and organization of convection is required. This study examines the role of mixing and entrainment in modulating CSA, highlighting the impact of different turbulence parameterizations on convection organization using WRF model.

Multiple idealized Radiative-Convective Equilibrium (RCE) simulations, designed to replicate the atmospheric conditions of the Greater Houston Area, are conducted by varying the turbulence closure. Compared to 3D-Smagorinsky simulations, both 1D-YSU and YSU-2D-Smagorinsky produced too many small cloud systems with shorter lifetime. A similar trend was observed for August 2022 real simulations over the Greater Houston Area, where convection is a dominant process. We attribute this contrast in size distribution to the sensitivity of cloud organization to entrainment processes and mixing length. Specifically, increasing the horizontal mixing length in YSU-2D-Smagorinsky simulations enhanced CSA, leading to the formation of larger, more persistent cloud systems. The findings of this study are useful to improve diffusion parameterizations in NWP models, particularly for CSA modeling.

Oral Presentations - SR1 634

Breno Goldenberg Araujo (MS)

Differentiating turbidites and contourites in a Miocene-Pleistocene deep-water drift deposit, offshore West Antarctica

The advance and retreat of ice sheets play a crucial role in driving sediments off the continental shelf break. The work presented here leverages the extraordinary interglacial-glacial sedimentary archive preserved in cores U1532 and U1533 from IODP Expedition 379, recovered from the continental rise in the Amundsen Sea offshore West Antarctica. The study focuses on the Late Miocene to Pleistocene sedimentary record, specifically the Middle Pliocene interval (approximately 4.2–4.8 million years ago).

A key hypothesis is that turbidites dominate during glacial periods, when ice sheets advance to the shelf break, increasing downslope sediment transport. Turbidites, characterized by sharp erosional bases, graded bedding, and poorly sorted textures, indicate rapid sedimentation during glacial periods when ice reaches the shelf break, enhancing sediment transport downslope. An opposing hypothesis is that the study site is sufficiently distal from the primary source that contourites, shaped by persistent bottom currents, prevail even during glacial periods. Contourites, identified by continuous fine laminations, bioturbation, and better sorting, are associated with sustained bottom-current activity, and tend to dominate during interglacial periods when ice retreat reduces downslope sediment transport.

The primary objective of this study is to distinguish between turbidites and contourites to better understand whether the glacial periods are recorded in this record and to understand the environmental significance.

Determining the dominant depositional regime across glacial and interglacial periods at this locality will provide crucial insights into the interplay between ice-sheet dynamics, ocean circulation, and sedimentary processes on the Antarctic continental rise.

Alexei Ignatiev (MS)

Cretaceous opening of the Canada Basin (High Arctic): New Constraints from regional gravity and magnetic data

The Canada Basin (also known as the Beaufort Sea) covers an area the size of the Iberian Peninsula (476,000 km2), remains frozen over most of the year, and is bordered by Canada (Northwest Territories, Yukon) and the USA (Alaska). Previous seismic refraction studies have shown that the 340-km-wide, east-west dimension of the deepest water area - with a maximum water depth of 4683 meters - is underlain by oceanic crust ranging in thickness from 4-7 km that is roughly symmetrical about a curvilinear, north-south-trending spreading ridge marked by a linear, gravity low. The Mesozoic opening history of the Beaufort Sea has remained controversial as it has relied on geologic data from the plate margins with less integration of geophysical data from the rifted margins and oceanic crust: Hypothesis 1 proposed that the northern Alaskan and Arctic Canadian margins are rifted, conjugate margins; this model requires a large, 70° degree, counterclockwise rotation of Arctic Canada to restore it to the margin of Alaska; and Hypothesis 2 proposed that the Northwind Ridge west of the Beaufort Sea is a strike-slip margin that accommodated early opening while the Alaskan rifted margin formed during a second opening phase. In this presentation, I use regional gravity and magnetic data tied to seismic reflection and refraction data to improve the structural and geologic interpretations of the three margins of the triangular Canada Basin: 1) the steeper, arcuate, and more narrow Alaskan margin is a transform boundary characterized by linear and steeply-dipping faults; 2) the gently sloped, wider, and straighter margins of the Northwind Ridge to the west and Eastern Canada are rifted, continental margins defined by discontinuous, seaward-dipping, low-angle normal faults; and 3) opening of the triangular-shaped Canada basin occurred in a protracted rift phase (Late Jurassic-Albian) followed by a period of slow, oceanic spreading during the Late Cretaceous about a pole of rotation located north of the basin.

Poster Presentations

1 - Nirvan Abhilash (PhD)

Physics-Informed Neural Networks for Rainfall Nowcasting : A Hybrid Data-Physics Approach

This study presents a novel methodology for rainfall prediction over the Indian peninsula using Physics-Informed Neural Networks (PINNs). We develop a hybrid model that combines data-driven deep learning with physical constraints derived from the advection-diffusion equation. The model integrates ERA5 reanalysis data, including 10m wind components (u10, v10) and total precipitation, to predict rainfall patterns across the region spanning 5-50°N and 60-110°E. Our neural network architecture employs multiple hidden layers with GELU activation functions, batch normalization, and dropout regularization to capture complex spatiotemporal relationships. The key innovation lies in the custom loss function that balances traditional mean squared error with physics-based constraints, enforcing consistency with atmospheric fluid dynamics principles. We implement a gradual increase in the physics loss weighting during training to enhance model stability. The methodology incorporates finite difference schemes to compute spatial and temporal derivatives for the physics-informed component. Our approach represents an important step toward integrating domain knowledge with machine learning techniques for meteorological applications, potentially improving prediction capabilities beyond traditional data-driven or purely physical modeling approaches. This framework offers promising opportunities for enhanced rainfall forecasting in regions characterized by complex monsoon dynamics and topographical influences.

2 - Amna Afzal (PhD)

Microplastic Detection in Complex Environmental Matrices: Comparative Study of Thermal Degradation Methods

Detecting and analyzing MPs in complex environmental samples often requires extensive sample workup, which can affect the reliability of results through sample loss and introduction of allochthonous contamination, in addition to reducing the analytical throughput and efficiency. To address these challenges, this study explores thermal degradation techniques—Rock-Eval and Pyrolysis Gas Chromatography-Mass Spectrometry (Pyrolysis GC-MS)—as methods for detecting and characterizing MPs without the need for sample preparation. The goal is to determine the minimum detection and identification thresholds for MPs in complex environmental matrices using these approaches.

To assess the effectiveness of both methods, polystyrene and polyethylene microplastics were spiked into soil, sediment, and sand matrices at concentrations ranging from 0.00034% to 4.2%. Both Pyrolysis GC-MS and Rock-Eval were used to analyze the samples, with lower concentrations tested more cautiously on Pyrolysis GC-MS to prevent instrument contamination.
The results show distinct differences in the sensitivity and accuracy of the two methods. While both techniques successfully identified MPs, pyrolysis GC-MS demonstrated greater sensitivity, detecting MPs at concentrations as low as 0.00034%. In contrast, Rock-Eval was more effective at higher concentrations (1% to 4.2%), showing a linear increase in Total Organic Carbon (TOC) with increasing MPs content. These findings highlight the limitations of Rock-Eval for low-level detection and emphasize the precision and reliability of pyrolysis GC-MS in identifying MPs, even at trace levels. This study underscores the importance of method selection for microplastic analysis and supports the use of pyrolysis GC-MS in developing standardized protocols for environmental monitoring. The findings contribute to improving the accuracy and comparability of microplastic research across various environmental matrices.

Poster Presentations

3 - Jumoke Akinpelu (PhD)

Crustal structure characterization offshore Niger Delta, Nigeria: impact on hydrocarbon exploration in ultra-deepwater

The Niger Delta Basin, Nigeria is a well-established and highly productive petroleum province with production mainly from well-explored Cenozoic plays in the inland, coastal, and slope fairways. The steady decline in production raises the question of whether deeper water plays based on Cretaceous source rocks can provide the path to increased production. This study integrates deeply penetrating regional 2D seismic reflection data, gravity, magnetic and well data for the 300,000 km2 on- and offshore area of the Niger Delta Basin. The objective of this study is to determine the crustal types underlying the 10-18 km thick basin and their influence on source rock maturation and hydrocarbon potential across all areas of the delta. Three types of crust were identified: 1) continental crust (CC), characterized by extensive, orogenic-related magnetic anomalies; 2) proto-oceanic crust (POC), which displays weakly developed fracture zones; and 3) oceanic crust (OC), characterized by well-developed fracture zones and spreading anomalies. Two-dimensional gravity modeling shows that the POC exhibits widely varying gravity anomalies, indicating the presence of localized blocks of the exhumed mantle and volcanic rocks in this broad transition area between the necking zone of continental crust and normal oceanic crust formed along an organized spreading ridge. Seismic data show that continental rifts extend 120 km seaward of the previous COB and newly identified tracts of POC crust with low radiogenic heat flow underlie 75% of the Niger Delta Basin. Aptian-Albian plate reconstructions of the protruding continental promontory of eastern Brazil provide a good pre-rift fit with the deeply recessed COB in the Niger Delta area. The 1D basin models in this study integrate these observations on crustal thickness variations, radiogenic heat production, and overburden thicknesses to predict that Aptian-Albian to Early Paleocene source rocks within continental rifts are in the oil window.

4 - Claudia Aramburu Tinoco (Undergrad)

Monitoring Spatiotemporal Variability of Suspended Sediment in Texas Coastal Systems Using In-Situ Measurements and Hyperspectral Imaging

Texas coastal wetlands and estuaries are crucial in mitigating inland damage from storm surges and flooding—events expected to increase due to climate change. However, these ecosystems face threats from sea level rise (SLR), subsidence, and coastal erosion, disrupting sediment dynamics. As land subsides and sea levels rise, erosion accelerates, reshaping coastlines and altering sediment distribution. If sediment supply cannot offset these losses, wetlands degrade, reducing their ability to stabilize shorelines and buffer against further erosion. Monitoring total suspended solids (TSS) is essential for understanding these changes and their effects on water quality, bathymetry, and ecosystem resilience. While satellite multispectral imagery has been used to measure water quality, its limitations hinder accuracy. Hyperspectral imaging, with additional spectral channels, improves TSS retrieval. This project examines spatiotemporal TSS and salinity variability in Trinity and Matagorda Bay, focusing on areas that may experience bathymetric changes due to sediment deposition or erosion. We consider factors like river discharge, tides, and waves using USGS and NOAA data. TSS is measured through in-situ water samples, salinity and temperature profiles via a CTD, and bathymetry via single-beam sonar. Our data reveal spatial and seasonal TSS trends influenced by natural processes and suggest potential anthropogenic impacts near the Intracoastal Waterway in Matagorda Bay. These findings highlight sediment transport pathway complexity, and the need for long-term monitoring. Additionally, using hyperspectral imaging to track TSS during flood stages will improve our understanding of sediment transport during high-discharge events. Our TSS models, with finer temporal resolution, can provide valuable insights for land management officials, including collaborators at the Texas Water Development Board (TWDB), to support reservoir operations and sediment management strategies.

Poster Presentations

5 - Muhammad Asif (PhD)

Constraining Orogen-Parallel Extension in the Central Himalayas: Insights from InSAR Time-Series on the Dangardzong Fault

The Dangardzong Fault (DF) in the Nepal Himalayas is an extensional fault that accommodates orogen-parallel extension. Although slip rates exist for many faults that accommodate Himalayan orogen-parallel extension, none exist for the DF, despite several decades of research on this prominent rift-bounding structure. In this study, we employed small-baseline subset interferometric synthetic aperture radar time-series analysis to investigate the surface displacement patterns across the DF. The results reveal a dominant east-west extensional surface displacement, with significant horizontal and vertical components across the fault zone. An 11-kilometer-long InSAR swath profile yields an estimated fault slip rate of 2.3 ± 0.5 mm/yr across the DF, indicating low active orogen-parallel deformation rates, consistent with the regional kinematics of southern Tibet. This extension rate is an order of magnitude faster than the orogen-parallel extension rate estimated from geologic data (~0.22 mm/yr) on the DF since 10 Ma.

West of the DF the slip rate on the Talphi fault is 2.8 mm/yr, the Gurla Mandhata detachment 100 km west accommodates ≥5 mm/yr of orogen-parallel extension, and further west the Karakoram fault accommodates ~7 mm/yr of orogen-parallel extension. This pattern reveals a westward increase in the rate of orogen-parallel extension. I interpret this pattern as arising from oblique convergence. Analysis of GPS data from the Himalaya shows that in the Mt. Everest region, at 86.9°E where the angle of obliquity is ~0°, the orogen-parallel component of the velocity field is negligible. Westward, the orogen-parallel component of the geodetic velocity field increases to ~2 cm and an angle of obliquity of ~10°.

6 - Tarryn Aucamp (PhD)

Unraveling Olympus Mons: Lava Flows, Surface Evolution and Geologic Mapping

Unlike Earth, where plate tectonics shift volcanic hotspots over time, Mars' stationary lithosphere has sustained volcanism in fixed locations over billions of years. Lower heat flow, gravity and atmospheric pressure contributed to the formation of extensive volcanic provinces like Tharsis and Elysium, which remain well-preserved due the absence of plate tectonics, surface water and significant weathering processes. The Tharsis volcanic province is one of the most remarkable regions on Mars, covering ~25% of Mars' surface and home to Olympus Mons–the largest volcano in the Solar System. Rising 21.1 km above the Martian datum, Olympus Mons is a massive shield volcano with a basal width of ~550 km and surface area of ~250 000 km2. Its formation began in the late Noachian to early Hesperian (~3.6 Ga; Werner et al., 2009), with eruptions persisting into the late Amazonian (~230 Ma; Robbins et al., 2011) and possibly as recently as 50 Ma (Neukum et al., 2004). Thus, Olympus Mons provides an ideal site to investigate prolonged volcanism, mantle evolution, and large-scale volcanic features.

This study uses Mars Orbiter Laser Altimeter (MOLA), Context Camera (CTX), and High-Resolution Imaging Science Experiment (HiRISE) data to identify and classify lava flows, volcanic features, and mass-wasting deposits on Olympus Mons and its surrounding aureole deposit. The objectives are to: 1) develop a catalog of lava flows and volcanic features, 2) compare identified features to terrestrial analogs, 3) refine the geological map of this region after Tanaka et al. (2014), and 4) combine spatial analyses with Compact Reconnaissance Imaging Spectrometer for Mars (CRISM) compositional data. By integrating knowledge gained through martian meteorite studies with orbital observations of volcanic provinces on Mars and remote sensing of Earth's volcanic landscapes, this research provides a comprehensive view of Olympus Mons' volcanic history and its implications for Mars' geologic evolution.

Poster Presentations

7 - Ruth Beltran (PhD)

Crustal structure and structural evolution of the Brazilian rifted passive margin in the Campos basin, Brazil

The Barremian/Aptian rifted-passive margin of the Campos basin, Brazil, is 320-km-wide and is underlain by two sub-parallel rift zones: 1) the Internal rift is located in water depths of 80 -1500 meters; 2) the External rift is located in water depths of 2600-3200 meters. The structural style in the Campos Basin consists of a Miocene to recent passive margin fold belt, characterized by an updip normal detachment surface at the base of Aptian salt, with overlying thin-skinned, extensional salt tectonics. Below this normal detachment, the Aptian-rift-related basement structure consists of horsts and grabens. Previous research has focused on characterizing rift systems on the continental slope; however, this study presents an integrated analysis of the most distal, deepwater areas within the rift system. I use a 3D gravity inversion model to characterize the crustal density values for: 1) the highly thinned continental crust, with density values between 2.65 and 2.67 g/cm3; 2) continental crust modified by magmatism, with density values between 2.71 and 2.75 g/cm3; and 3) normal oceanic crust in the ultra-deepwater area of the External rift with a density of 2.85 g/cm3. I then interpret 3D seismic cubes in the External rift zone to define a hyperextended, External rift domain characterized by a thick sequence of syn-rift carbonate rocks, with scattered igneous sills, capped by an extensive, late Barremian sag sequence with potential source rocks exhibiting shale lithologies similar to those of the Internal Rift. Using these data, I generated 1D basin models based on four pseudo-wells distributed across the External rift. As a result of the basin modeling, the pre-salt stratigraphic units are predicted to reach the top of the oil window at a depth of 4 km. The post-salt section located in the deepest mini basins of the External rift is predicted to reach the top of the oil window at a depth of ~3000 km.

8 - Kyra Bennett (MS)

A chemometric machine learning framework for oil classification: A California case study

Chemometrics is a powerful tool for the oil industry, enabling effective analysis of complex geochemical data related to reservoir characterization, exploration, and production optimization. In this study, we used a published dataset from Peters et al. (2008) to develop our own chemometric decision tree model for classifying California oils, seeps, tar balls, and source-rock extracts.

Initial observations from the Peters et al. (2008) dataset show that several features include outliers with unusually high values such as C26/Tet, PAH-RI, and C29H/H, while other features such as $\delta^{13}C$ displayed unusually low values. Correlation analysis revealed strong positive relationships between SC2D/SC2P and SC3D/SC3P (r2 = 0.95), and between C29H/H and G/H (r2 = 0.93). The strongest negative correlations were between SC2D/SC2P and C24/C23TT, as well as SC3D/SC3P and C24/C23TT (both r2 = -0.77).

The decision tree model achieved ~91% accuracy on the training data, with a training error of ~9% and a validation error of ~32.9%, indicating potential overfitting due to the limited sample size. Feature importance analysis identified BNH/H as the most influential variable, followed by SC3D/SC3P.

Building on this workflow, we will apply the model to an expanded set of 82 California oil samples using GC-MS/MS to obtain high-resolution biomarker data. In addition to the conventional biomarker ratios, the updated workflow incorporates unconventional biomarkers such as diamondoids to improve the classification of oil families. We will also test and compare other machine-learning approaches to identify the most effective algorithms for oil classification.

Poster Presentations

9 - Ashish Bhattarai (PhD)

Evaluating WRF-CAMx Model Performance in Simulating Surface Ozone During Different Sky Conditions in Houston, Texas

Accurately simulating surface ozone concentration remains challenging, partly due to uncertainties associated with cloud simulations. This study evaluates the biases in surface ozone concentrations simulated by using the Weather and Research and Forecasting model (WRF) and the Comprehensive Air Quality Model with Extensions (CAMx) across Houston, Texas, for the periods of September 2021 and 2022. We employed the cumulative distribution function (CDF) to stratify sky conditions at each grid cell, based on the Cloud Optical Depth, simulated by WRF and observed by Advanced Baseline Imager (ABI) onboard Geostationary Operational Environmental Satellite (GOES – 16). This enabled us to examine the differences in modeled and observed frequencies of clear and cloudy conditions, enabling an assessment of how inaccuracies in cloud simulations are associated with biases in ozone simulations. In September 2021, monitoring sites experienced clear skies for 39% and 43% of the time, according to the observations and simulations, respectively, with corresponding positive bias of ~ 9 ppb. In September 2022, clear sky occurrences increased to 56% in the observations and 47% in the simulations, followed by a reduced bias of ~ 6.5 ppb. Inter-annual variation in ozone concentrations showed consistent patterns between observations and simulations. From 2021 to 2022, an increase in clear sky occurrences from 39% to 56% corresponded to an increase in observed ozone concentrations by ~ 7 ppb. Similarly, an increase in clear sky occurrences from 43% to 47% was linked to a 4.5 ppb higher modeled ozone concentration. In both years, the model and observed ozone align more closely, showing higher correlations and lower mean bias on clear days than on cloudy days. These findings highlight the limited representation of clouds can substantially contribute to biases in simulating surface ozone concentrations, emphasizing the need to improve cloud simulations to enhance model accuracy.

10 - Nathaniel Brunello (Undergrad)

Investigations into the deformation history of the Cutoff Formation, SE New Mexico

The Cutoff Formation (Permian), part of the Guadalupian reef complex of the Delaware basin of west Texas and SE New Mexico, contains extensive networks of calcite-filled fractures; cross-cutting relationships suggest at least three generations of fracture development. During the FIELDGeo 2025 Winter Trip, we collected seven samples of calcite-filled fractures from an outcrop of the Williams Ranch Member of the Cutoff Formation along US highway 62-180, south of Guadalupe Mountains National Park. Samples are spiculitic mudstone/wackestone with several orientations of calcite-filled fractures; these were selected to investigate the age of deformation, tectonic history, and fluid migration in the area. Calcite in the fractures varies from euhedral crystals with individual grains up to 4 mm across to “dirty” fine-grain veins barely distinguishable from the surrounding rock. Near-vertical fractures striking 128 to 148 dominate the calcite-filled fractures in outcrop. These fractures, up to 15 mm wide, exhibit generational bands of euhedral calcite and fluoresce white, yellow, and orange under UV. Other near-vertical fractures filled with large calcite crystals strike 114, 071 and fluoresce yellow under UV. Smaller near-horizontal fractures with fine-grained calcite converge into a 25 mm wide fracture which fluoresces yellow and blue-white under UV. Samples were processed to produce sections for fluid inclusion analysis and laser ablation inductively coupled plasma mass spectrometry (LA-ICPMS) analysis. Fluid inclusion analysis will determine the fluid composition, temperature, and pressure of inclusion formation conditions. Future research will occur at the University of Kansas, where LA-ICPMS will determine the trace element composition of the calcite. Data from LA-ICPMS will be used in U-Pb isotope analyses to constrain the geologic age of the observed deformation, thus contributing to the body of knowledge on the diagenetic evolution of the Delaware Basin.

Poster Presentations

11 - Abigail Cantoni (PhD)

Detrital zircon from Mars: trapped sediment components in the highly shocked shergottite northwest Africa 11509

NWA 11509 is a 500-gram meteorite found in Mali. It is classified as a Martian Shergottite which is one of the classifications of Achondrites. An achondrite is a stone from a differentiated body such as Earth or Mars. It is identified as Martian through its ΔO17 value which falls on the Mars fractionation line. Shergottites are ultra-mafic intrusive rocks that have ages ranging from 0.15 to 2.4 Ga and source compositions that can range from enriched with respect to REE (rare earth elements) or depleted (Udry et. al. 2020).

This specific stone is a coarse grained gabbroic intermediate shergottite with heavily shocked features from the ejection event and the fall to Earth. Despite the categories enriched, intermediate and depleted, all shergottites are very similar to chondrites (early solar system materials) or depleted with respect to them. Given this information, all shergottites should not be enriched enough with zirconium to form zircon, however, zircon was found on the interior of the meteorite and identified along the Mars fractionation line.

The zircons were found specifically within the vesicles of the meteorite. This points to the possibility that these zircons were captured by wind-blown sediments on Mars but does not fully explain how they formed. Zircons were found in a similar fashion in the meteorite NWA 7034 and its parings (Costa et. al. 2020). NWA 7034 is a polymictic breccia with zircon grains found within the mafic clasts (Costa et. al. 2020). In order to form zircons, large amounts of fractional crystallization must have occurred which we don't see much evidence of on the surface. Since NWA 11509 is a gabbroic shergottite, it must have been brought to the surface due to some process to catch the wind-blown sediment. More work is needed to understand these surface processes and internal magmatic processes on Mars.

13 - Patrick Casbeer (MS)

Manganese phase identification and oxidation state assessment in analog sample analysis at Mars-evolved gas analyzer measurements

Manganese (Mn) enrichments in Gale Crater, Mars, have been identified by the Curiosity rover in fracture fills, coatings, and nodules. However, the oxidation state and phase of Mn is unresolved. This could provide insights about Mar's paleoenvironmental conditions, aqueous alteration, and redox potential. This project aims to determine Mn phases and oxidation states by comparing laboratory analog data with Sample Analysis at Mars (SAM) evolved gas analysis (EGA) data. 40 samples total were analyzed: natural Mn-rich sediments, ores, nodules; pure, synthetic Mn phases. Laboratory thermal gravimetry (TG), differential scanning calorimetry (DSC), and SAM-like EGA were performed and compared to SAM-EGA releases from Mars. Laboratory X-ray diffraction (XRD) was performed to determine phase identifications and phase abundances. Mn2+-carbonates evolved CO2 between 400-650 °C, a range similar to siderite and magnesite. Hydrous Mn and Fe phosphates evolved H2O across a broad temperature range, but their signals are likely to be obscured by releases from absorbed water, hydrated salts, or amorphous phases. Mn sulfate and sulfide evolved SO2 potentially within SAM's upper temperature limit of 870°C. Mn2+ oxides did not evolve O2, whereas Mn3+-oxides evolved O2 between 515-1000°C and Mn4+-oxides evolved O2 between 460-1000°C. The lack of evolved O2 in some Gale Crater drill samples suggests not only the absence of oxychlorine species but also the absence of Mn3+/Mn4+ Mn oxides. This indicates that Any Mn oxides in Gale Crater drill samples without evolved O2 must be Mn(II) oxides. Mn2+ oxide could form in reducing conditions without oxidants, challenging previous assumptions that strong oxidants were necessary for the Mn detections.

Poster Presentations

14 - Juan Cruz (Undergrad)

Investigating SWS Parameters Preceding the 2009 Mw 6.1 L'Aquila Earthquake

The 2009 L'Aquila Earthquake resulted in hundreds of deaths and caused tens of thousands to become homeless. It also prompted the indictment of Italian seismologists who were monitoring the activity leading to the earthquake for not alerting the public despite increased seismic activity. The successful prediction of earthquakes remains elusive as the change in earthquake activity alone is not a reliable precursor condition. A promising method of stress condition monitoring is the use of shear wave splitting (SWS). SWS parameters (delay time and fast direction) are sensitive to the crack density in the crust, which is supposed to increase before a large earthquake. Precursor events in the months leading to the L' Aquila earthquake were used to analyze spatial and temporal changes in SWS parameters. The data was sourced from the ORFEUS data center and SWS parameters were obtained from the filtered and processed data using a modified semiautomated MATLAB code (Robinson et al., 2020). These parameters will be analyzed spatially and temporally in the context of the faulting in the L'Aquila region leading up to the main Mw 6.1 event.

15 - Rijul Dimri (PhD)

Graph Neural Network-based PM2.5 concentration estimation and forecasting

Accurate forecast of PM2.5 concentration is crucial as it equips governments with essential data for public health alerts and assists policymakers in decision-making processes. In air quality modeling, achieving a reliable model accuracy has been often challenging due to uncertainties in input parameters and the oversimplification of chemical mechanisms. Despite extensive earlier efforts to incorporate machine learning and numerical weather prediction and air quality models, there is still a room for improvement in better capturing spatiotemporal information of atmosphere across non-uniform and non-Euclidean spaces. To fill such a gap, in this study, we propose an Adaptive Graph Attention Network (AGAT)-based deep learning framework to bias-correct PM2.5 concentration estimated by a numerical model, which can further improve the forecast accuracy. Leveraging masked self-attentional layers, the AGAT incorporates spatial information along with the temporal features to bias-correct CMAQ-simulated PM2.5 concentrations. The graph nodes are generated based on air quality monitoring stations in Korea, each characterized by 47 features, and then graph structure adaptively learns the spatial relationships among the stations to build node connections, taking advantage of attention mechanism. We then implement causal dilated 1D convolution (TCN) to capture long term (24-hrs) temporal dependencies among the features for each station to bias-correct PM2.5 concentrations for 72 hours. This framework achieves significant accuracy across 183 stations in Korea, with an Index of Agreement (IOA) of 94.7%, 78.6%, and 77.3% for forecasting hours of day 1, 2, and 3, respectively with improvements in IOA by 26.2%, 10.7%, and 9.7% for the corresponding days.

Poster Presentations

16 - Amberlee Enger (MS)

Using Isotope Forensics to Solve the Case of Carbonation and Serpentinization of Modern Oceanic Peridotites from the Vavilov Basin, Mediterranean Sea

Hydrothermal alteration of mafic minerals occurs when seawater percolates through seafloor basalts and peridotites at elevated temperatures (100-500°C) [1]. The high abundance of olivine in peridotites leads to dramatically different hydrothermal reactions than for typical basaltic crust, generating high pH fluids, serpentine minerals, hydrous minerals, iron oxides, and carbonates. Given that serpentinization reactions are highly conducive to the precipitation of carbonates, significant efforts are underway to optimize carbon sequestration efforts in ultramafic tailings [2]. Carbonate formation in natural serpentinite systems remains underexplored, which hinders our understanding of modern geochemical cycles linking the atmosphere, oceans, and solid Earth. The sources of carbon and major cations in peridotite-hosted carbonates, along with reaction temperatures and rates of serpentinization and carbonation, remain uncertain.

To address these questions, we have obtained 18 peridotite samples (~3 Ma) from a recent oceanic drilling campaign in the Vavilov basin, Mediterranean Sea (IODP Exp. 402), where normal faulting has allowed for infiltration of seawater and hydrothermal alteration [3].We will analyze major and trace element abundances (by EPMA) and follow with δ44Ca, δ18O, and 87Sr/86Sr analyses in silicate and carbonate phases from these samples. This combination of isotopic proxies will allow us to evaluate the sources of Sr and Ca in the silicates and carbonates, the temperatures at which they formed, and the reaction rates involved. Additionally, Ca isotopes in peridotite-hosted carbonates are severely underexplored (often assumed to have similar δ44Ca to sedimentary carbonates), so our data will have strong implications for the use of δ44Ca as a carbonate recycling proxy in mantle-derived igneous rocks [4].
[1] Allen & Seyfried, 2004 [2] Stokreef et al., 2022 [3] Sanfilippo et al., 2025 [4] Antonelli & Simon, 2020

17 - Morgann Farley (Undergrad)

Sediment Budget Investigation of Longyearelva in Longyearbyen, Svalbard

Longyearelva is a dynamic fluvial system that is fueled by glacial meltwaters and starts as a braided river that rapidly changes into a single straight channel. Historically, Longyearelva was uncontrolled and meandered freely through Longyeardalen (Norwegian, 1938). The current presentation of this river was designed to protect the town of Longyearbyen from flooding and erosion (Løvaas, 2021). As the glaciers retreat, their meltwaters supply sediment into the channel. The sediment washes out from beneath the glaciers and from the moraines. However, rain events could cause more erosion of the riverbed or valley walls. Suspended sediment samples were taken along the length of the river using ISCOs and grab samples to obtain a clearer picture of the where dominant sediment source is. Graphs compare upstream versus downstream sediment fluctuation. Additional graphs compare the weather conditions to explain variations in sediment discharge. Peak sediment discharge occurred at 15:00; the lowest sediment discharge occurs at 05:00. Longyearbreen and Larsbreen have almost equal suspended sediment discharge. The additional sediment concentration can be attributed to erosion from the river channel or aeolian derived sediments. During weather events, sediment recorded downstream was higher than corresponding upstream measurements, indicating that sediment is being sourced from additional locations.

Poster Presentations

18 - Zachary Guess (MS)

A Critical Evaluation of the Young Moon Hypothesis: Radiogenic Ca and Sr isotope constrains on the contentious relationship between anorthosite and pyroxenite lithologies in 60025

The Moon is thought to have formed through a large collision between the proto-Earth and a Mars-sized impactor. The tremendous energy released led to vaporization of both bodies, vigorous mixing, and subsequent condensation of the Earth and Moon (Fu et al, 2023). Initially the Moon was largely molten, but crystallization led to the formation of the white colored Lunar Highlands. The highland crust is composed primarily of anorthite, with minor pigeonite, high-Ca pyroxene, and ilmenite (Ryder, 1982). After formation of the highlands, another large impact (related to the South Pole-Aitken Basin) is thought to have caused a rapid overturn of the lunar mantle, leading to large-scale depressurization melting, and emplacement of darker-colored pyroxenitic melts within the previously formed anorthositic crust (Zhang et al. 2022).

Based on multiple isotopic dating methods, the oldest parts of the moon (the highlands) are thought to have formed at 4.44 Ga (Sossi et al. 2024). A much younger age (4.36 Ga), however, has been suggested based on Pb-Pb and Sm-Nd analyses of clasts coming from sample 60025 (Borg et al, 2011). This young age for the moon is highly contentious and has significant implications for the geochemical evolution of the Earth-Moon system but may be based on the invalid assumption that the pyroxenite and anorthite components comprising sample 60025 were formed at the same time. We prdict that the "Young Moon" age is actually the age of the pyroxenitic clasts, and not of the older anorthosites. In order to validate this hypothesis, we will use radiogenic Ca and Sr isotope variations in the pyroxenitic and anorthositic clasts to test whether the two lithologies formed in isotopic equilibrium. If the two lithologies formed at the same time from a single reservoir, they will have an identical (within uncertainty) initial value for ε40Ca and 87Sr/86Sr. We are currently validating our methodology on small plagioclase grains (<1mg) from the Stillwater Complex.

19 - Nilay Gungor (PhD)

Seismic Insights into Deep-Water Stratigraphy and Reservoir Potential in the Mahanadi Basin, India

The Mahanadi Basin, located on India's east coast, is a divergent basin of considerable geological interest and hydrocarbon potential. This study investigates the large- scale facies distributions, stratigraphic, and structural framework of deep-water deposits in the Mahanadi Basin using 2D and 3D seismic data, well logs, and well reports. Our main objective is to interpret the depositional settings of the deep-water deposits and document their evolution. Key stratigraphic horizons, unconformities, and the basement are mapped from 3D seismic surveys to better understand the spatial distribution of facies. Seismic attributes, mainly RMS amplitude, dip angle/azimuth, and instantaneous frequency are employed to highlight geological features like channel margins, sand bodies, levee/overbank deposits, and channel geometries, which may indicate potential hydrocarbon accumulation zones. Preliminary findings reveal the presence of progradational clinoforms, numerous channels with high sinuosity, turbidites, and mass transport deposits (MTDs). The Plio- Miocene section is considerably thicker toward the NE part of the basin and includes several channel complexes. Seismic attribute analysis highlights the younger part of the stratigraphic section which has numerous Miocene-aged channels and sand bodies mostly in the southeastern part of the 3D seismic area. The lower part of the section is characterized by chaotic and smaller channels. Deep-marine, highly sinuous channel systems, characterized by migrating meander loops, channel scour, and fill elements, were interpreted to reflect turbidity current activity. Geological and geophysical analyses of deep-water sediments and system tracts provide insights into the depositional architecture evolution and hydrocarbon prospectivity in the region.

Poster Presentations

20 - Rashik Islam (PhD)

Deep Learning-Based PM Forecasting and Post-Infant Mortality Assessment in Urban Areas: A Case Study in Bangladesh

The study investigated the application of advanced deep learning models for forecasting air pollution and assessing its associated health impacts in Bangladesh. Specifically, the Temporal Fusion Transformer (TFT), Deep Autoregressive Recurrent Neural Network (DeepAR), Generative Adversarial Network (GAN), and 1D Convolutional Neural Network (1D-CNN) were employed to forecast daily PM2.5 concentrations for the next seven days across four urban areas (Chattogram, Rajshahi, Dhaka, and Sylhet) during 2013–2018. The study further quantified post-infant mortality risks attributable to PM10 exposure in these regions. Model performance was evaluated using Mean Absolute Error (MAE), Root Mean Square Error (RMSE), Coefficient of Determination (R^2), and Index of Agreement (IOA). Among the models, TFT demonstrated superior forecasting capability, achieving a mean RMSE of 21.23 μg/m³, which was 48.1% lower than DeepAR (34.81 μg/m³) and significantly better than 1D-CNN (40.59 μg/m³) and GAN (40.90 μg/m³). The attention mechanism in TFT effectively captured complex temporal and non-linear relationships in PM2.5 data, while feature relevance analysis highlighted PM10, temperature, and relative humidity as key predictors. Health risk analysis, conducted using the World Health Organization's (WHO) Air Quality Health Impact Assessment Tool (AirQ+), revealed significant post-infant mortality impacts, with the highest attributable mortality proportions per 100 population observed in Dhaka (42.95%) and Sylhet (24.64%). The strong agreement between observed and forecasted health outcomes underscored the reliability of the TFT model. These findings provide a robust framework for improving air quality management and informing public health policies to mitigate the adverse effects of particulate matter exposure in Bangladesh.

21 - Sui Jia (PhD)

Metamorphic history and detrital provenance of the Torbashi thrust sheet, Eastern Pamir, and their tectonic significance

The northward subduction of the Paleo-Tethys ocean resulted in the development of the Karakul–Mazar terrane along the southern margin of the Asian continent during the closure of the Paleo-Tethys ocean in late Triassic to early Jurassic. Previous studies presented different ages for the lithologies in the Torbashi thrust sheet. Igneous zircon ages of 198 to 206 Ma imply the continued magmatism and deformation during or after the collisional event (Imercke et al, 2019), while other studies suggest a contradictory peak metamorphism age varying from ca. 250–220 Ma (Yang et al., 2010) to ca. 200–180 Ma (Zhang et al., 2018). This study aims to understand the provenance and P–T–t conditions of samples from the Torbashi Thrust sheet through zircon U–Pb dating and petrographic modeling of bulk rock analyses. Our preliminary results reveal that the western Karakul-Mazar terrane reached peak metamorphic conditions of 600-650 °C, 4-5 kbar (~15-18 km) at ~200 Ma. We accordingly conclude that crustal thickening of the overriding Karakul-Mazar terrane during final collision in the Early Jurassic drove peak metamorphism. This event was terminated by rapid breakoff of the Paleo-Tethys slab following collision. Detrital zircon signatures from samples indicate the Torbashi thrust sheet is a part of the Karakul-Mazar Terrane with age clusters of 200 to 230 Ma, and the possible provenance of the sediments are from the adjacent Late Triassic Karakul–Mazar plutons and the southern margin of Asia, with age clustered 400 to 900 Ma (a pronounced peak in ~550 Ma).

Poster Presentations

22 - Sagun Gopal Kayastha (PhD)

A Deep Learning Framework for Satellite-Derived Surface PM 2.5 Estimation: Enhancing Spatial Analysis in the United States

Monitoring fine particulate matter (PM2.5) is crucial for evaluating air quality and its effects on public health. However, the limited distribution of monitoring stations presents a challenge in accurately assessing air pollution, especially in areas distant from these stations. To address this challenge, our study introduces a two-step deep learning approach for estimating daily gap-free surface PM2.5 concentrations across the contiguous United States (CONUS) from 2018 to 2022, with a spatial resolution of 4 km. In the first phase, we employ a depthwise-partial convolutional neural network (DW-PCNN) to fill gaps between surface PM2.5 stations, utilizing aerosol optical depth (AOD) data from the Moderate Resolution Imaging Spectroradiometer (MODIS). In the second phase, we integrate the PM2.5 grids imputed by the DW-PCNN with meteorological and anthropogenic variables into a deep convolutional neural network (Deep-CNN) to further enhance the accuracy of our estimation. This enables us to estimate gap-free surface PM2.5 concentrations accurately, evidenced by Pearson's correlation coefficient R of 0.92 and an index of agreement (IOA) of 0.96 in 10-fold cross validation. We also introduce a grid-based method for calculating PM2.5 design values (DVs), providing a continuous spatial representation of PM2.5 DV that enhances the traditional station-based approach. Our grid-based DV representations offer a comprehensive perspective on air quality, facilitating more detailed analysis. Furthermore, our model's ability to provide spatiotemporally consistent, gap-free PM2.5 data addresses the issue of missing values, supporting health impact research, policy formulation, and the accuracy of environmental assessments.

23 - Nima Khorshidian (PhD)

Investigating Aerosol–Cloud Interactions over Houston Using Advanced WRF-Chem Schemes

In this study, the influence of anthropogenic emissions and aerosol properties on air quality and cloud formation over Houston was investigated using the Weather Research and Forecasting model coupled with Chemistry (WRF-Chem). The objective was to examine how variations in emission strength affect the composition of fine particulate matter ($PM_{2.5}$) and cloud-related microphysical processes in an urban environment.

A series of high-resolution simulations was performed using the Spectral Bin Microphysics (SBM) scheme, CBMZ gas-phase chemistry, and the MOSAIC aerosol module. Anthropogenic emissions were systematically scaled across different scenarios (0x, baseline, 2x, and 5x) to assess the sensitivity of aerosol concentrations and cloud microphysics to emission intensity. Detailed aerosol chemistry and microphysical representations were utilized to enable a comprehensive evaluation of atmospheric responses to different pollution levels.

Time–height profiles were generated over a defined urban subregion to analyze the vertical distribution of total aerosol mass and cloud-relevant variables. Through this approach, insights were gained into how aerosol composition influence cloud development under varying emission conditions.

This work contributes to the advancement of urban air quality modeling by providing a framework for assessing emission impacts on aerosol–cloud interactions. The methods and findings presented may support future efforts aimed at improving predictive capabilities for urban pollution and its role in weather and climate processes.

Poster Presentations

24 - Emily Klang, Avery Narhi (Undergrad)

An Investigation of the Aeolian Transport Mechanisms That Form Lomas in the Rio Grande Delta

The Rio Grande is a river system along the Texas-Mexico border that flows into the Gulf of Mexico. River avulsions along the Rio Grande have created abandoned channels, which serve as sediment sources for aeolian features known as lomas, composed of mainly silt-sized particles. Given the sediments are fine-grained, the lomas are expected to form far from the sediment source. However, these landforms are located adjacent to the abandoned deltaic floodplains, suggesting unknown formation mechanisms. The proximity of the lomas to their sediment source suggests that silt transport and deposition may occur for particle aggregates rather than individual grains. In this study, we investigate the mechanisms of particle transport and deposition that build lomas. To do this, we will characterize wind speed and direction, as well as the grain size and sediment cohesion. We will deploy 3 sediment traps oriented with the dominant wind direction, from the lake edge to the lomas. With the traps, 3 anemometers at varying heights will be used to measure wind velocity profiles, providing a basis for understanding aeolian sediment transport dynamics. Sediment samples collected will be analyzed for grain size distribution using a CILAS 1190 laser particle size analyzer. To investigate the mode of transport and cohesion, we will examine the samples with a microscope. Wind velocity data, grain size analysis, and cohesion parameters, will then be used in sediment transport equations to estimate the critical and near-bed shear shear stresses required to begin sediment transport. We expect that the silt-sized particles are transported as aggregates that allow for the formation of lomas in close proximity to the sediment source. The topography of the Rio Grande Delta is shaped by lomas, which also host critical infrastructure such as roads. As deltas are dynamic environments, understanding the processes that rework deltaic sediment is crucial for interpreting how these landscapes evolve.

25 - Raymond Kwaku Twumasi Oware (PhD)

Evaluating E3SM Global Storm-Resolving Model Simulations of Deep Convection: Insights from DP-SCREAM during TRACER

Global Storm-Resolving Models (GSRMs) are becoming increasingly vital for advancing climate modeling and improving the prediction of extreme weather events. Houston, a coastal region frequently affected by deep convective storms, offers an ideal setting to evaluate the ability of GSRMs to simulate deep convection. This study assesses the performance of the Doubly Periodic Simple Cloud-Resolving E3SM Atmosphere Model (DP-SCREAM) using observations from the TRacking Aerosol Convection Interactions Experiment (TRACER) campaign. DP-SCREAM effectively reproduces the diurnal cycles of clouds and precipitation, demonstrating much greater skill than the E3SM single column model. The performance of DP-SCREAM is not degraded on days with distinctive sea or bay-breeze circulations, suggesting that the DP-SCREAM is applicable to coastal regions, partially due to the forcing datasets already capturing the influence of breezes. DP-SCREAM also replicates biases persistent in the global version of SCREAM: the underrepresentation of boundary layer shallow clouds, a lack of mid-level congestus clouds, and the popcorn convection, characterized by small and disorganized convective cells generating the strongest precipitation. To investigate these issues, two sensitivity experiments were conducted: increasing the mixing length and scaling up the buoyancy flux within the Simplified Higher Order Closure scheme. Increasing the mixing length improved mid-level congestus representation and reduced unrealistic early morning fog occurrence. Enhancing buoyancy flux only marginally improved the bias of underproduced big convective cells. An additional resolution sensitivity test at 0.5 km demonstrated that a refined horizontal resolution alone is insufficient to resolve these biases.

Poster Presentations

26 - Syd Lineberry (Undergrad)

Using Thermochronology to understand fault movement, with special consideration of the Granite Pass fault, Little Hatchet Mountains, NM

Thermochronology combines an understanding of radioactivity and diffusion to determine the thermal history of rocks. As minerals cool, below their "closure temperature", the isotopic clock is started as daughter products begin to be retained. Measuring the time scale of the dropping temperatures of a rock can then be correlated to the movement of a rock unit within a fault system. In normal faults the foot wall cools as a result of fault slip removing the rocks above. In thrust systems, the hanging wall moves so as to create topographic highs, which are then subject to enhanced erosion and subsequent cooling.

The Granite Pass-Windmill thrust system in the Little Hatchet Mountains, SE New Mexico placed a Precambrian rapakivi granite over an overturned unit of Pennsylvanian Horquilla limestone. Previous U-Pb geochronologic data extracted from zircons from the rapakivi granite date the unit at 1.1 billion years old. We aim to use thermochronologic methods on this rock to establish an exhumation history for the Granite Pass-Windmill thrust system. We collected several samples of the rapakivi granite from the Little Hatchet Mountains on the FIELDGeo 2025 Winter Trip. These samples show the classic rapakivi texture of porphyritic potassium feldspar phenocrysts mantled by plagioclase feldspar, and they also contain a significant proportion of mafic minerals, primarily hornblende. Samples were processed via heavy liquid separation aiming to isolate apatite crystals from the granitic body. We plan to analyze these apatite grains using the fission-track and He-He methods to be presented at GSA.

27 - Melania D. Maqway (PhD)

The Isola Dike, Northwest Italy: Evidence for Carbonatite Metasomatism in the Lower Continental Crust of the Ivrea-Verbano Zone (IVZ), Southern Alps

Metasomatism is key in transferring volatiles and metals between the subcontinental lithospheric mantle (SCLM) and the lower crust, influencing crustal evolution and generating economically valuable mineral deposits. Carbonatites (>50 wt% carbonates) are particularly effective metasomatic agents, exploiting fracture networks to disseminate volatiles that modify the SCLM. These processes are significant in understanding alkali magmatism, mantle metasomatism, and mantle–crust heterogeneity (Beccaluva et al., 1992; Griffin et al., 1988; Kogiso et al., 2004). Despite frequent consideration of carbonatite in metasomatic models, their specific sources, nature, composition, and role in deep crustal processes remain inadequately constrained. This study presents new data on the Isola carbonatite-wehrlitic dike emplaced at the base of the mafic complex in the Ivrea-Verbano Zone (IVZ), Southern Alps.

The dike comprises clinopyroxene cumulates (~50 modal %) and interstitial calcite (~20 modal %); minor to accessory phases include plagioclase, Fe-Ti oxides, apatite, titanite, scapolite, vesuvianite, and clinozoisite, reflecting silicate–carbonatite magma interaction. Diopside composition enriched in Ca–Al–Ti and CO2 - rich scapolite indicates post-emplacement hydrothermal overprinting during Alpine exhumation processes. Trace element patterns enrichment in LREE, Nb, Th, U, Pb, and depletion in K, Ta, and P are typical of cumulate carbonatites from a subduction-modified, volatile-rich SCLM. These findings emphasize the role of metasomatic fluids in lower crustal settings and encourage further investigation into the potential for REE mineralization in the Ivrea-Verbano Zone.

Poster Presentations

28 - Daniel Maya (PhD)

Crustal structure and basin modeling of Cretaceous source rocks in deepwater settings

Since 2022, hydrocarbon discoveries along Namibia's deepwater margin have raised questions about similar accumulations in Uruguay. I have utilized 2D and 3D seismic reflection to refine the understanding of the crustal structure in deepwater Uruguay, which is characterized by the obliquely oriented, 41-km-wide and 90-km-long Rio de la Plata rift that offsets the otherwise continuous, 80-140-km-wide belt of seaward-dipping reflectors of Hauterivian age. I combine crustal data to create 1D predictive hydrocarbon basin models from three source rock horizons across various upper-slope and deep-water settings on the Uruguay margin. Our results include: 1) I predict dry gas in the 3.4-km-thick sedimentary section over the upper slope of the 26-km-thick crust near the Gaviotin-1 well, which shows documented dry gas from Jurassic source rock; 2) I predict condensate from Aptian source rocks and oil maturity for Cenomanian-Turonian source rocks in the 5.5-km-thick sedimentary section over the 12-km-thick crust of the Rio de la Plata rift; 3) I predict a wet gas window for the Aptian source and an oil window for Cenomanian-Turonian rocks on the lower slope over a 6-km-thick crust of the outer SDR belt near the Raya-1 well; and 4) I predict a dry-to-wet gas window maturity for Aptian source rocks and oil maturity for Cenomanian-Turonian rocks in the depocenter of the Rio de la Plata rift's 3-km-thick crust. Aptian source rocks are gas-prone due to 4-8 km sedimentary overburden on the Uruguay margin. Younger Cenomanian-Turonian source rocks, with 3-3.4 km of overburden, show gas and oil maturity in all crustal provinces, including the Rio de la Plata rift. This predicted zone of Aptian deepwater maturity suggests the possibility of up-dip migration into Albian (110-100 Ma) turbiditic and Campanian-Santonian (86-72 Ma) contouritic reservoirs.

29 - Jack McLaughlin (MS)

Evaluating the Use of Clay and Groundwater Chemistry to Differentiate Fluvial Versus Marine Sediments in an Oil Field Setting, Focused on the Frio Formation of the Texas Gulf Coast

A new methodology exists that allows the cation composition of clays to be determined by analyzing the chemical composition of water which is based on the instantaneous water/rock reaction of cation exchange. This has been used to evaluate the environments of deposition of the sediments in the Chicot/Evangeline aquifers of the Texas Gulf Coast at shallow depths, but has never been used on deeper systems at elevated temperatures. The purpose of this study is to use this methodology to evaluate much deeper sediments in the Frio Formation to determine if it is valid in different conditions.

Although it shares many similarities to the Chicot/Evangeline aquifers, the Frio Formation is deeper, older, and has been subjected to higher temperatures. Exchange constants are not available at elevated temperatures, so they must be calculated using thermodynamic data. Therefore, a thermodynamic database of heats of reaction for relevant exchange reactions is required. Once exchange constants are generated, clay cation composition can be calculated and used to gain insight into the system.

This study will evaluate if using the relative abundance of mole fractions of cations can help to determine the environment of deposition of clay sediments, as shown in the Chicot/Evangeline aquifers. Additionally, the identification of compartmentalization within fields, hydrodynamics of the system, and the controlling effects of water versus rock on cation composition will be evaluated.

One of the primary contributions of this study is a completed, internally consistent thermodynamic database of heats of reaction for exchange reactions that can be used to calculate reasonable exchange constants at elevated temperatures in future work.

Poster Presentations

30 - Joshua Miller (MS)

3D seismic stratigraphy and tectonic controls on contourite and turbidite sedimentation along the deepwater Atlantic margin of Uruguay

In this study, we combine three, depth-converted 3D seismic reflection volumes totaling 22,984 km2 with 10,000 km of regional 2D seismic lines from the slope of the South Atlantic margin of Uruguay. Using this dataset, structural maps in depth were made using five horizons (Eocene, Danian, Campanian, Albian, and Aptian) aps. Paleoscan software was applied to all major horizons to improve the imaging of geobodies such as channel complexes, fan deposits, play fairways, and source rock extent. Based on their distinctive seismic facies and 3D geometries, I divide the 3-km-thick Albian-Paleocene section into three facies associations: 1) Turbidite facies from Albian-Cenomanian include 116-long and 37 km wide submarine fans with thicknesses ranging from 500 to 1500 m characterized by symmetrical, channel-levee systems. Seismic facies include low-amplitude and continuous progradational reflectors that down lap onto high amplitude reflectors and exhibit lobe geometries. This period of gravity-driven turbidite deposition occurred during the early opening phase of the South Atlantic from (120-100 Ma) when bottom currents were not yet established. 2) Mixed turbidite-contourite facies from Cenomanian-Maastrichtian (100-66 Ma) are characterized by asymmetrical, channel-drift systems. Seismic facies include low-high amplitude agraddational and progradational chaotic-continuous reflectors. This period of contour current-driven re-deposition occurred during the intermediate opening phase of the South Atlantic and is 1000-2500 meters thick. 3) Contourite facies from Maastrichtian-Late Paleocene (66-56 Ma) characterized by asymmetrical, channel-drift systems which include elongated drifts and a moat. Seismic facies include low-high amplitude agraddational and progradational continuous reflectors. This period of strong contour current-driven re-deposition occurred during the more recent opening phase of the South Atlantic and is 500-2000 meters thick.

31 - Pauline Nguyen (Undergrad)

Assessing Organic Carbon Pools in Coastal Prairie Soils

Carbon Capture, Utilization, and Storage (CCUS) is a growing field aimed at reducing carbon emissions. Nature-based solutions like soil carbon storage are especially promising for their cost-effectiveness and scalability. This study evaluates coastal prairie soils at the University of Houston Coastal Center (UHCC) in La Marque, Texas, for their potential as long-term carbon sinks.
We collected 35 soil samples from various prairie conditions, ranging from high-quality native vegetation to degraded areas affected by invasive Chinese Tallow, a former military base, and an active oil rig. Environmental variables like vegetation type, ground cover, and soil composition were noted at each site. Samples were taken from both topsoil (0–30 cm) and subsoil (100–120 cm), freeze-dried, homogenized, and ground to grain sizes <2 mm and <250 μm.

Total Organic Carbon (TOC) was measured using ramped pyrolysis with an initial temperature of 200°C and a heating rate of 30° C/min (Disnar et al., 2003). This method allowed us to estimate both active and stable carbon pools by analyzing thermal decomposition profiles. Preliminary data from 10 samples showed TOC values ranging from 0.20% to 2.22%, with variation linked to depth and site conditions.

We used pyrolysis parameters S1 (labile carbon) and S2 (resistant carbon) to assess carbon stability. S1 values were low (0.03–0.09 mg HC/g rock), suggesting limited short-term carbon. S2 values ranged from 0.35 to 2.95 mg HC/g rock, reflecting broader variability in long-term storage potential.

Remaining samples are being analyzed with the same method and supplemented by Pyrolysis-Gas Chromatography (Py-GC) for molecular-level insights. This helps explore links between TOC stability, vegetation cover, land use, and soil depth.

Poster Presentations

32 - Oriyomi Ojelabi (MS)

Shallow subsurface mapping of Evergreen Cemetery using non-invasive geophysical methods

The Evergreen Negro Cemetery is believed to be one of the oldest African American cemeteries in Houston. The cemetery burials date from 1887 to 1950 and are mostly unmarked. Geophysical surveys are great noninvasive techniques to map the subsurface without digging. We use high-resolution 3D GPR and magnetic surveys to investigate the unmarked grave in the Evergreen Negro Cemetery in Houston, Texas. These geophysical methods use high-frequency radio waves to illuminate subsurface objects and measure the variations in the Earth's magnetic field, respectively. For the geometry of the GPR and Magnetic surveys, we designed a very dense 3D grid of 6×6 meters area where the grid consisted of 25 parallel lines spaced with line spacing of 25 centimeters for both the X-axis (E-W direction) and the Y-axis (N-S direction) to acquire high-resolution GPR and magnetic data. GPR's data shows a series of reflections at shallow depths (0.1 – 0.3 meters) across the survey grid, marking the metallic and concrete headstones. Strong reflections of old graves are more identifiable at 4 ft in the GPR section with a convex upward shape. Magnetic surveys show high anomalies above the buried headstones and low magnetic intensity over the burials. This study aids in historical documentation and preservation of unmarked burials, which can benefit the families by connecting them to their deceased ancestors and a chance to pay homage to their ancestors. The integrated GPR and Magnetic survey provides significant information about the subsurface locations of the lost headstones and the unmarked burials for the Evergreen Negro Cemetery.

33 - Abe Okayli Masaryk (PhD)

Deep earthquakes and association with carbonate equilibrium melting conditions

Deep earthquakes, below 300 km, provide insight to the dynamics of subduction zones, yet their triggering mechanisms are debated. In this study, we compare the depth distributions of deep earthquakes from various subduction zones with inferred pressure-temperature (P-T) conditions, namely the lithostatic pressure and the 410-km seismic discontinuity. The peak depths of these earthquake distributions are mapped to P-T conditions using standard geophysical models. Following Thompson et al. (2016), we correlate these peaks with the carbonate solidus curve to identify potential thermal or compositional triggers. Limited by its correlative nature, this approach offers a rapid assessment of seismic-geochemical interactions in subduction zones. Fits to generalized Gamma, generalized Pareto, and other distributions are compared, where the best-fit model may hint at processes shaping depth patterns. We discuss how equilibrium mineral phase assumptions in a non-equilibrium system may limit insights, introducing a carbonate-driven hypothesis alongside the metastable olivine model.

Poster Presentations

34 - Jake Parsons (PhD)

Seismic monitoring of underground hydrogen storage

Hydrogen will play an important role in improving energy security and lowering emissions in the United States. Increasing hydrogen utilization calls for large scale storage of hydrogen gas. The most proposed storage method is within preexisting subsurface domains, such as depleted oil/gas reservoirs and saline aquifers, whose high porosity, accompanied by a low porosity caprock, makes them ideal candidates for large scale hydrogen storage. However, to ensure safe and efficient operations, methods for monitoring subsurface hydrogen are required. We demonstrate the efficacy of seismic monitoring methods for subsurface hydrogen applications by running fluid flow simulations for injection and production cycles in several reservoir types, converting the results into seismic wave speed and density models using established rock physics equations, and simulating seismic reflection surveys via SPECFEM2D. We then analyze the synthetic seismograms and identify differences between production cycles to track the hydrogen plume location in the subsurface reservoir.

35 - Anuska Pudasaini (PhD)

Fingerprinting Meltwater Facies in Pleistocene to Recent Sediments in the Amundsen Sea, West Antarctica

The Amundsen Sea sector of Antarctica has long been considered the most vulnerable part of the West Antarctic Ice Sheet (WAIS). Meltwater discharge has been documented from Thwaites Glacier but little is known about its variability over time. The sedimentary record provides an opportunity to study meltwater discharge over both space and time, and thus could shed light on glacial behavior today and in the future. International Ocean Discovery Program (IODP) Expedition 379 completed two drill sites on the continental rise of the Amundsen Sea that provide almost-continuous cores from the seafloor to the upper Miocene, records unavailable on the shelf. However, it is not certain that meltwater plumes can be traced that far. This study aims (1) to clarify past interpretations of the meltwater facies proximal to Thwaites glacier and (2) to study sedimentary records in IODP 379 cores to determine if the facies can be found in the distal record.

Poster Presentations

36 - Ali Raza (PhD)

Decoding stalagmites composition — a non destructive approach

Stalagmites are an excellent natural archive for reconstructing past climate and environmental conditions. We applied hyperspectral imaging (HSI), a non-destructive technique, to remotely characterize their composition. This method was initially tested on Stalagmite MAJ-4 from Madagascar. Spectral indices were used on shortwave infrared images for mineral detection and mapping. An X-ray diffraction (XRD) analysis was conducted to validate the spectral results, and elemental analysis was carried out to understand mineral-element relationships. To evaluate the reproducibility of our approach, we analyzed more stalagmites from Trapiá and Furna Nova caves in Brazil.

Results from spectral indices show that aragonite dominates the upper part of Stalagmite MAJ-4 (0-105 mm depth), except between 35–45 mm, where calcite is more prevalent. In the lower part (105–130 mm), calcite dominates. Indices values from both (aragonite and calcite index) show a strong agreement with phase percentages of corresponding minerals obtained from XRD. We observed a strong correlation between Strontium (Sr) and aragonite, with Sr/Ca ratios serving as a marker for mineralogical transitions.

By linking these mineralogical and geochemical variations to past environmental conditions, our approach supports robust paleoclimate reconstructions. For example, variations in mineral phases can indicate shifts in hydroclimate (wet vs. dry conditions). Similarly, trace element signatures provide insights into paleo-flood events, prior carbonate precipitation, and even anthropogenic or volcanic influences.

37 - Robby Reyna (MS)

Applying machine learning techniques to the classification of groundwater contamination within a natural carbon dioxide reservoir

In eastern-central Utah a natural CO2 reservoir leaks brine and CO2 into overlying formations and to the surface in the form of geysers and seeps. Brine and CO2 originate from deep, Pennsylvanian aged hydrocarbon formations and migrate upward through faults and fault damage-zones. Along the path of upwelling, shallow aquifers such as the Jurassic Navajo and Entrada Sandstones act as intermediate reservoirs before the solution migrates up-dip or through overlying fractures. Groundwater wells in the area allow for the chemical characteristics of both Navajo and Entrada Sandstones to be obtained. Additionally, there are over 100 surface water analyses available from literature which have been collected from the handful of geysers and seeps.

The establishment of methods to detect and map CO2-driven brine upwelling in shallow aquifers is imperative as more geologic carbon storage projects begin operation. The purpose of this study is to utilize unsupervised machine learning techniques such as principal component analysis (PCA) and K-means clustering to group analyses based on the extent of brine impact and identify areas of possible upwelling. There are presently no results for this study; however, it is expected that results will be obtained prior to poster presentation.

It is expected that PCA will eliminate dimensions within the data which do not change significantly with the introduction of CO2-rich brine. This will leave between 3 and 5 principal components which conserve most of the data variability. Next, K-means clustering will utilize statistics to assign centroids to data clusters which are expected to represent varying levels of brine contamination. The product will be a contour map highlighting the variable impact brine upwelling and contamination have on the area, possibly pointing to unrecognized areas of upwelling and associated hidden fractures.

Poster Presentations

38 - Estefani Ruiz Toro (MS)

Tectonic origin of the Bering Sea from geophysical and geological constraints

The Bering Sea, covering approximately 2,000,000 km² with an average water depth of 1.5 km, remains one of Earth's most extensive and least understood oceanic basins. Previous tectonic hypotheses suggest its formation resulted from 1) Paleogene back-arc spreading along the Aleutian Arc and 2) Paleogene entrapment of pre-existing, North Pacific normal oceanic or oceanic plateau crust followed by subduction initiation along the Eocene to Recent Aleutian volcanic arc. To test these hypotheses, I integrate various geophysical methods to determine the age and crustal thickness of the Bering Sea along with the age and style of structural deformation along its margins in western Alaska and eastern Russia. Results include: 1) Gravity: A regional 3D gravity inversion was conducted to estimate crustal thickness and Moho depth variations. The initial isostatic Moho depth was calculated using Airy isostasy with constraints from regional refraction and reflection profiles. Sediment thickness variations were accounted for using a regional density model. The final model resulted in a crustal thickness range of 13–33 km, consistent with an oceanic plateau origin; 2) Magnetics: Compilation of existing magnetic data shows regional north-south trends that are at a high angle to both magnetic basement trends along the northern margin of the Bering Sea and those along its southern margin with the Aleutian arc. No age information can be extracted from these anomalies. This regional pattern does not support its back-arc origin behind the Aleutian arc 3) Heat flow: Heat flow measurements indicate a Middle Eocene (45 Ma) age of origin; 4) Depth to basement: These measurements also support a Paleogene age (55-40 Ma); and 5) Style of deformation of the Bering Sea margins: These data are compiled from previous seismic reflection and outcrop studies and are consistent with collision of an intra-oceanic arc in Paleogene time (55-40 Ma).

39 - Bilge Sasmaz (MS)

Development of Mechanical Earth Model and Stress Analysis at the HFTS-1 Site, Midland Basin

Unconventional reservoirs like the Wolfcamp Shale in the Permian Basin have low permeability,making hydraulic fracturing essential for economic production.Effective hydraulic fracture design depends on accurate estimates of pore pressure and in situ stress. Currently, two main methods are used to estimate in situ stress: the poroelastic approach (Thiercelin and Plumb, 1991; Savage et al., 1992) and the viscoelastic stress relaxation model (Kohli and Zoback, 2021; Singh and Zoback, 2022). This study compares these two methods using extensive field data from Hydraulic Fracture Test Site 1 (HFTS-1) located in Reagan County, Texas.Due to the different mechanical properties of rocks with high and low carbonate content, a significant variation in stress as a function of depth is expected with important implications for the propagation of hydraulic fractures in such sediments. Minimum horizontal stress computed using the poroelastic approach with measured fracture closure and reopening pressures acquired using diagnostic formation integrity tests. A significant variation in the minimum horizontal stress is observed. Each of these approaches is used to build a Mechanical Earth Model (MEM).A MEM integrates well logs, image logs, and stress data to characterize the subsurface mechanical properties and fracture responses under varying stress conditions. It allows stress distribution and rock failure mechanisms for the various stratigraphic units to be predicted. The MEMs offer the required geomechanical framework to support hydraulic fracture design, wellbore stability, low-frequency DAS monitoring responses, and reservoir performance evaluation. The two modeling approaches will then be compared with available hydraulic fracture and microseismic data to assess their predictive capabilities and practical implications. This comparison is expected to provide valuable recommendations for optimized fracture modeling and reservoir development strategies in unconventional reservoirs.

Poster Presentations

40 - Margaret Sauer (Undergrad)

U-Pb Calcite Geochronology and Fluid Inclusion Analysis of the Earp Formation: Insights into Laramide Deformation in the Little Hatchet Mountains, SW New Mexico

The Earp Formation (Permian) in the Little Hatchet Mountains in SW New Mexico contains conglomerate, sandstone, and limestone strata. In the southern portion of the range, limestone units are found within the complex Windmill-Granite Pass fault zone of Clinkscales and Lawton (2017), which is thought to be a major Laramide structure in the region. This project will focus on using the Earp to better understand the movement of this fault by two methods: fluid inclusions and U-Pb dating of calcite-filled fractures. Three samples of Earp limestone rich in deformed calcite-filled fractures were collected from the hanging wall of an imbricate thrust splaying off the main Windmill fault. Samples are dark grey wackestone with 1mm size quartz micro-nodules throughout and are cut by a network of fine calcite-filled fractures. Fractures are primarily 0.5-2 mm in thickness, but range from 5mm to nearly indistinguishable hairline fractures. The calcite in these veins occurs as very fine, white, sugary crystals. 100 micron thick sections were produced for laser ablation inductively coupled plasma mass spectrometry (LA-ICPMS) U-Pb geochronology and fluid inclusion analysis. These data will be used to better understand the age of deformation and determine the digenetic history of the Earp formation in the region around Windmill fault. This will contribute to our understanding of the tectonic history of the Little Hatchet Mountains.

41 - Peter Savrides (MS)

Crustal structure, tectonostratigraphy, and hydrocarbon potential of the deepwater, rifted-passive margin of Nova Scotia

The rifted-passive margin of Nova Scotia straddles the area between the northern non-volcanic rifted margin of Newfoundland and Labrador and the southern volcanic-rifted margin along the eastern USA. Most of the previous 210 wells drilled in the offshore area of Nova Scotia have targeted the more accessible upper slope (0.10-1km BSL) that includes section of a massive, 1-2km thick, late Jurassic-Cretaceous carbonate margin. Drilling in the shallow water area, and more recently with several widely spaced wells in the lower slope and abyssal plain (~5 km BSL), have mainly proven unsuccessful mainly due to poor source rock maturity. The hypotheses of this study include: 1) deep marine, clastic Late Jurassic source rocks are of higher quality than those equivalent, carbonate facies in shallow water as observed along other Atlantic margins such as Guyana; 2) hydrocarbon maturation is focused on the non-volcanic marginal rift as observed on the Moroccan conjugate margin; and 3) mature Jurassic source rocks extend onto the adjacent oceanic crust as previous studies have shown in Morocco. This study integrates seismic horizons tied to deepwater wells, well stratigraphy and geochemical data on source rocks, heat flow data, the lithosphere-asthenosphere boundary, crustal thickness, salt thickness and remobilization, and paleowater depths to predict lateral variations in the thermal history of the Late Jurassic source rocks (0.6-0.7% VroEq) using the ExCalibur basin modeling software. The resulting basin models calibrated using documented oil and gas shows from previous drilling results, along with supplemental Gammacerane geochemical data from offshore Morocco and Portugal, have revealed new undrilled deepwater areas of a mature Sinemurian-Pliensbachian-Toarcian source rock complex in Nova Scotia.

Poster Presentations

42 - Kenneth Shipper (PhD)

Regional maturation model for hydrocarbons along the Guyana-Suriname margin based on improved estimates of the thickness and thermal structure of the rifted lithosphere

The thermal structure of the lithosphere controls the variability of kerogen maturation along rifted margins. This study integrates seismic data, wells, and potential fields to model crustal thickness, lithosphere- asthenosphere boundary (LAB) depth, and radiogenic heat production from the Guyana- Suriname margin. We develop a new method to model the lithosphere' s thermal structure by estimating elastic thickness. Our model is validated using data from gas and oil wells in the region. Model inputs for our 3D basin model include: 1) mapping stratigraphic horizons from the Tithonian to the seafloor using KPSTM seismic reflection data provided by TGS, covering 51677 km2 of the Stabroeck block; 2) constructing 1D basin models from temperature data of seven wells tied to the seismic grid; 3) modeling the Moho through gravity inversion; 4) calculating LAB based on elastic thickness estimates of 42-75 km along the thinned continental crust.

Using the imaged crustal structure, we built a regional 3D basin model with ExCaliber, a fast basin simulator utilizing machine learning to solve the transient heat flow equation. The model includes the top and base of the Canje Formation as source rock acmes. Thermal maturity of the Canje Formation matches predicted maturity of many shelf- slope oil fields with standard thermal stress (STS) ranging from 84-220 °C. Thermal maturity increases towards the southeast near the Guyana-Suriname maritime boundary and the Demerara Plateau, validated by the distribution of condensate fields and gas shows, including several shelf and slope oil fields within the condensate window (>135 °C STS). Predicted maturity at the base of the Canje Formation extends thermal maturity 48 km northeast onto the late Jurassic oceanic crust of the deep Guyana basin. Jurassic source rocks achieve thermal maturity as far as 50 km from the Demerara Plateau shelf edge, with Aptian source rocks extending within a few km of the A2-1 well.

43 - Kaylin Tunnell (PhD)

Mineral chemistry of olivine from chondritic meteorite compared to Martian and 4-Vesta meteorites – implications for the evolution of extra-terrestrial rocky bodies

Although olivine is an important constituent of many mafic and ultramafic rocks, its trace element composition in terrestrial and extra-terrestrial systems remains understudied. Here we present the preliminary results of a study that investigates the trace element chemistry of olivine in a series of meteorites, i.e., the Martian meteorites ALHA 77005 and NWA 7397, the 4-Vesta meteorite NWA 5480 and the chondrite Ausson. The Martian meteorites were previously suggested to be poikilitic shergottites implying that these rocks underwent partial melting. The 4-Vesta meteorite is classified as a harzburgitic diogenite that underwent multiple deformation events. Ausson is an ordinary chondrite.

Petrographic observations show that all samples are composed of olivine, orthopyroxene, clinopyroxene with locally abundant plagioclase and chromium-rich spinel; rare pyrrhotite was found in NWA 7397. Electron microprobe analysis of olivine shows that forsterite content (Fo = molar [Mg/(Mg+Fe)] *100) is generally between Fo = 70-73, although grains from the Martian meteorite NWA 7397 have lower values of Fo ~60. Nickel contents are <100 ppm Ni in olivine from Ausson and NWA 5480, whereas the Martian olivines contain between 200 and 600 ppm Ni. It is noted that Ni does not correlate with Fo in the presented data. Manganese content displays a distinct negative correlation with Fo ranging from 4500 to 7500 ppm Mn. Laser ablation ICP-MS analysis of olivine from ALHA 77005 and Ausson yield similar trace element patterns when normalized to the composition of the Bulk Silicate Earth (BSE). Implications for progressive evolution seen in trace element chemistry.

Poster Presentations

44 - Md Upal Shahriar (PhD)

Geophysical insights into tectonostratigraphic framework and hydrocarbon prospectivity in the Andaman Basin

The Andaman basin features various tectonic processes, including the oblique subduction of the Indian Oceanic plate, strike-slip sliver movement, and pull-apart development with a back-arc spreading center. This study integrates gravity, seismic reflection, and well data to clarify the tectonostratigraphic framework and hydrocarbon system. An analysis of potential fields and a seismic-derived top-of-basement map reveals basins formed from subduction and strike-slip movement along the Andaman-Nicobar Islands. The forearc basin serves as a narrow, deep sediment accumulation area. The Andaman pull-apart basin in the late Miocene emerged with a spreading ridge during the later stage of polyphase rifting in the Andaman Sea, which underlies an active trough-like sediment deposition zone, accompanied by an older trough indicating asymmetric rifting. Inverted rifts, like the Oligocene Bampo formation of the Sunda block, may host hydrocarbons in the southeastern Andaman basin. Mapping the mid-Miocene unconformity shows inversion-related deformation progressing from southeast to west in the southeastern Andaman basin, stemming from the Sumatra basin, where recent discoveries like Timpan and Larayan have been made. The breakup unconformity in the eastern Andaman basin reveals normal faults and inversion-related uplifts. The mid-Miocene to early Pliocene sequences demonstrate less deformation, suggesting low tectonic activity in this area. With slightly folded strata and footwall uplifts, these sequences provide effective hydrocarbon trapping mechanisms.

45 - Eugenia Velasco (MS)

Comparing two data filtering methods to differentiate between on-road vehicle plumes and background measurements

Mobile measurements cover large areas of interest and provide a comprehensive spatial evaluation of local air pollution. However, the data sampled can also be biased by direct on-road vehicle emissions, especially for primary pollutants. The ability to distinguish quickly and precisely between a plume and background levels is crucial for source identification of key species of interest. Baylor University's Mobile Air Quality Laboratory 2 (MAQL 2) was equipped with an extensive suite of air quality instrumentation and deployed to San Antonio, TX, during the spring 2021 San Antonio Field Study (SAFS). During this campaign, the MAQL 2 provided a month of trace gas, aerosol, and Volatile Organic Compounds (VOC) data measurements made in San Antonio's urban core and its surroundings. This study utilizes two data filtering algorithms, Density-Based Spatial Clustering of Applications with Noise (DBSCAN) Plume Detection Tool and State-Informed Background Removal (SIBaR) on trace gas measurements (carbon dioxide, nitrogen oxide, and nitrogen dioxide) to systematically distinguish on-road emission sources from background/regional levels. Both filtering methods identify periods when local sources' contributions were high during the time MAQL 2 was on the road. This study determines and compares the consistency and accuracy of each tool for the trace gases being analyzed. The quick identification of plumes and their sources helps to interpret on-road measurements, identify on-road emissions, allow for a better comparison to models, and aid in the evaluation of on-road chemistry.

Poster Presentations

46 - Haini Wang (PhD)

Re-estimating Moisture Source Contribution Anomalies in the 2011 Texas Extreme Drought Event Using the Two-Layer Dynamic Recycling Model (2L-DRM)

With global warming, extreme weather events are becoming more frequent. In 2011, Texas experienced its worst year-long drought, causing $7.6 billion in agricultural losses. As a key component and link in the Earth's hydrological cycle, water vapor plays a significant role in extreme precipitation and drought events. Despite extensive research, traditional moisture tracking relied on 1-layer models, which ignore the vertical shear of the atmosphere.

Recently, we applied both 1-layer and 2-layer ERA5-based Dynamic Recycling models (DRM) to re-estimate Texas' moisture sources (1979–2014). The 2-layer model revealed greater contributions from local land, the Gulf of Mexico, and remote land, with local land's impact more than doubling—reaching 2.5 times in July–August than 1-layer model. While the 1-layer model showed the Tropical Pacific dominating in May and the Tropical Atlantic (excluded Gulf of Mexico) in June–August.
Since the differences have been noticed, furthermore, we plan to use the 2L-DRM to re-examine the moisture source contribution anomalies to Texas in 2011 and compare with the 1L-DRM to better understand what have really caused such extreme drought event.

47 - Zhixiang Zhang (PhD)

A Real-Time Instrument for Monitoring Strain Variations

Structural health monitoring is crucial for ensuring the safety and longevity of buildings, particularly in seismically active regions or facilities subjected to continuous vibrations and stress. This study aims to measure building deformations in real time using strain sensors.

The proposed system consists of three main components: sensors, an edge data acquisition unit, and cloud computing. The sensors feature a 24-bit, dual-channel data collector with a 10 Hz sampling rate and are controlled by an ESP32 microcontroller equipped with Wi-Fi and Bluetooth capabilities. This setup enables continuous data transmission to the acquisition unit, which subsequently uploads the data to the cloud for analysis.

This technology has potential applications in seismic resilience assessment, long-term structural monitoring, and early warning systems. Future work will focus on improving data processing techniques and integrating this system with other monitoring methods to enhance accuracy and reliability.

Organizing Committee of the 2025 Student Research Conference

Morgann Farley (Undergrad) and Karissa Vermillion (PhD):
Co-chairs and lead organizers
Isabela Garcia (Undergrad): Organizer and editor of SRC program
Christi Sterna (PhD): Organizer

Special thanks to Antonious Douglas (EAS Assistant to the Chair), our EAS faculty advisors (Drs. Brandee Carlson and Paul Mann), and our EAS IT support (Jay Krishnan and Jason Ognosky)!

Thank you to all of the volunteer faculty and industry judges. This would not have been possible without you!

Esteban Fernandez Azparren (Chevron)

Dr. Richard Beauboeuf (RTB Geoscience)

Henry Campos (Shell)

Dr. Brandee Carlson (EAS)

Chuck Caughey (Marathon Oil, retired)

Julian Chenin (ROGII)

Dr. Peter Copeland (EAS)

Catie Donohue (Murphy Oil)

Laura Faulkenberry (CNOOC)

Ted Godo (Geodog Exploration)

Dr. Adam Goss (CNOOC)

Ken Green (ExxonMobil, retired)

Dr. Dan Hauptvogel (EAS)

Dr. Xun Jiang (EAS)

Katarina Jonke (BP)

Ademola Lanisa (Total Energies)

Dr. Tom Lapen (EAS)

Dr. Jiaxuan Li (EAS)

David Liner (Hilcorp)

Dr. Paul Mann (EAS)

Cristina Masarik (Chevron)

Dr. Daniel Minisini (ExxonMobil)

Dr. Jincheol Park (EAS)

Kailesh Patel (Total Energies)

Dr. Jagos Radovic (EAS)

Dr. Alex Robinson (EAS)

Dr. Will Struble (EAS)

Dr. Julia Wellner (EAS)

Lance Wilson (Dunn Exploration)

Dr. Youtong Zheng (EAS)

Thank you to all of the volunteers who have assisted with set up and take down. This would not have been possible without you!

Lunch Set Up
Albert Chen
Bilge Sasmaz

Event Take Down
Fnu Anshika
Asmara Lehrmann

Oral Presentation Coordinators
Karissa Vermillion
Isabela Garcia
Morgann Farley
Christi Sterna

We would also like to thank and acknowledge the College of Natural Science and Mathematics for their contributions to the 2025 Student Research Conference. Thank you for your support!

UNIVERSITY OF HOUSTON

COLLEGE OF NATURAL SCIENCE AND MATHEMATICS

Who Are We?

The Department of Earth and Atmospheric Sciences at the University of Houston has a wide range of research programs central to the earth sciences.

Air Pollution
Air Quality
Applied Geophysics
Applied Rock Physics
Atmospheric Science
Carbonate Petrology
Climatology
Geodynamics
GIS
Hydrology
Igneous Petrology
Inorganic Geochemistry
Isotope Geochemistry
Marine Geology
Micropaleontology
Potential Fields
Remote Sensing
Sedimentology
Seismology
Sequence Stratigraphy
Structural Geology
Tectonics
Thermochronology
Whole Earth Geophysics

The Department offers M.S. and Ph.D. degrees in Geology, Geophysics, and Atmospheric Sciences, B.S. degrees in Geology, Geophysics, Environmental Sciences, and Atmospheric Sciences, and a B.A. in Earth Sciences. Fieldwork is a major component of all degree programs. The Department also offers Professional M.S. programs in Petroleum Geology and Petroleum Geophysics that are offered at convenient hours for professional geoscientists working in industry or aspiring for a professional position within the petroleum industry.

CONTACT US

Department of Earth and Atmospheric Science
4800 Cullen Boulevard, Houston, Tx 77204
Phone: (713) 743-3399
Web: http://www.eas.uh.edu